[RADIOCARBON, VOL 28, No. 2B, 1986, P 980–1021]

RADIOCARBON AGE CALIBRATION OF MARINE SAMPLES BACK TO 9000 CAL YR BP

MINZE STUIVER*, G W PEARSON**, and TOM BRAZIUNAS*

INTRODUCTION

Calibration curves spanning several millennia are now available in this special issue of *RADIOCARBON.* These curves, nearly all derived from the ^{14}C age determinations of wood samples, are to be used for the age conversion of samples that were formed through use of atmospheric CO_2. When samples are formed in reservoirs (eg, lakes and oceans) that differ in specific ^{14}C content from the atmosphere, an age adjustment is needed because a conventional ^{14}C age, although taking into account ^{14}C (and ^{13}C) fractionation, does not correct for the difference in specific ^{14}C activity (Stuiver & Polach, 1977). The ^{14}C ages of samples grown in these environments are too old, and a reservoir age correction has to be applied. This phenomenon has been referred to as the reservoir effect (Stuiver & Polach, 1977).

The reservoir age, or apparent age, R(t) is here defined as the difference between conventional ^{14}C ages of samples grown contemporaneously in the atmosphere and the other carbon reservoir. R(t) is not constant (t = cal age) because the difference in reservoir and atmosphere ^{14}C specific activity is liable to change with changes in reservoir parameters (such as size of the carbon pool, input and output fluxes and exchange with the atmosphere) and atmospheric $\Delta^{14}C$ values. However, due to the lack of detailed information, a variable reservoir age correction usually cannot be applied, and the user of ^{14}C ages then resorts to the assumption of a constant reservoir age correction R* (*ie,* the reservoir ^{14}C specific activity is assumed to parallel atmospheric ^{14}C specific activity at all times). The reservoir age correction R* is obtained from the conventional ^{14}C age of reservoir samples of either historically known age, or of inferred known age (such as the uppermost portion of lake sediment). This approach is, of course, only a first order approximation. However, even though the resulting reservoir corrected ^{14}C age is not the ultimate in accuracy, the corrected ^{14}C age should be closer to the ^{14}C age of a contemporaneous wood sample than the uncorrected one.

The recent introduction of the dating of mg C samples through AMS (accelerator mass spectrometry) allows for an improved determination of variable reservoir ages R(t) in lakes because it is now possible to measure, at different depths, the age differences between 1) those plant macrofossils that were originally utilizing atmospheric $^{14}CO_2$, 2) lake carbonate, and 3) gyttja. The first study of this kind has been made for the sediments of a small closed basin of the Lobsingsee, Switzerland (Andrée *et al,* 1986b). Here the problem of reservoir age corrections can be avoided entirely if a sufficient number of macrofossils formed directly from atmospheric CO_2 can be found.

* Department of Geological Sciences and Quaternary Research Center, University of Washington, Seattle 98195
** Palaeoecology Centre, The Queens University of Belfast, Belfast, Northern Ireland

For small carbon reservoirs where the exchange rate with the atmosphere is dominant (eg, a shallow 10ha lake) the change in specific ^{14}C content may well parallel the observed change in atmospheric ^{14}C content. For other reservoirs, however, appreciable differences are possible. For instance, the top 75m of the ocean (well mixed due to wave action, etc) attenuates atmospheric decadal $\Delta^{14}C$ changes strongly due to its inertia in responding to atmospheric forcing, and the deep ocean lags appreciably in its response to long-term atmospheric ^{14}C change. The idea of a constant reservoir age correction R* is not tenable in this case.

The reservoir age of marine shells has been determined in the past from the conventional ^{14}C age of shells of known historic age (year AD X), after correcting for fossil fuel CO_2-induced ^{14}C age change in the mixed layer of the ocean (Mangerud & Gulliksen, 1975; Robinson & Thompson, 1981). This fossil fuel corrected ^{14}C age is then compared with the age of the sample, *ie,* 1950 − X, and the difference is the reservoir or apparent age. This procedure assumes constant atmospheric ^{14}C level, where calendar years and ^{14}C years are interchangeable. Thus, the reservoir age in this instance is the fossil fuel corrected shell ^{14}C age minus the ^{14}C age of a sample formed from atmospheric CO_2 in AD X.

Olsson (1980), in addition, discusses the ^{14}C ages of samples formed from atmospheric CO_2 of the 19th century, and compares these with the conventional shell ^{14}C ages. The difference again is the apparent or reservoir age. But, as noted by Olsson, "in this discussion, it has been tacitly assumed that the aim is to arrive at a reservoir effect that is not affected by short-term fluctuations of radiocarbon in the atmosphere."

Two avenues of age calibration are possible for a sample formed in a fluctuating ^{14}C environment. One is to derive the variable reservoir age R(t) in conventional ^{14}C years, apply this correction to obtain a reservoir corrected ^{14}C age, and then use the calibration curves valid for samples formed directly from atmospheric CO_2. The other is to produce a separate calibration curve that includes the variability in reservoir ages. Such a curve gives the conventional ^{14}C age minus a ΔR number (explained later on) *vs* the cal BP (cal AD/BC) age. We here follow the latter approach for marine samples.

A box-diffusion model as described by Oeschger *et al* (1975) was used to simulate global carbon exchange. We attribute the observed atmospheric $\Delta^{14}C$ variability of the last 9000 yr to solar (heliomagnetic) and geomagnetic modulation of the cosmic ray flux (Stuiver & Quay, 1980; Sternberg & Damon, 1983), and consider model parameter change induced by oceanic (climate) change to be negligible over this time interval (Andrée *et al,* 1986a). The observed atmospheric $\Delta^{14}C$ record is used to calculate the ^{14}C content of the mixed layer (top 75m) of the model ocean, and the model mixed layer ^{14}C ages are plotted *vs* cal AD/BC (cal BP) ages. The calibration curves are different from those given elsewhere in this issue because the ^{14}C ages are not directly measured but calculated from the atmospheric record through carbon reservoir modeling. The curves therefore not only reflect the original measuring uncertainty in the wood $\Delta^{14}C$ values that constitute the model input, but also uncertainties in model parameters.

THE GLOBAL CARBON MODEL

The atmospheric $\Delta^{14}C$ data used as input for the model span the AD 1950–7746 BC interval. A composite data set (Fig 1) was derived by combining the data of Stuiver and Pearson (1986) for the AD 1950–500 BC interval, of Pearson and Stuiver (1986) for 500–2490 BC, of Pearson *et al* (1986) for 2500–5210 BC, of Linick, Suess and Becker (1985) for 5219–5346 BC and 5818–5882 BC, of Stuiver *et al* (1986) for 5685–5815 BC, 6475–6552 BC, and 6574–7198 BC, of Kromer *et al* (1986) for 5908–6200 BC, 6279–6469 BC, and 7206–7746 BC, and of Linick *et al* (1986) for 5355–5675 BC and 6205–6275 BC. The Figure 1 data represent average $\Delta^{14}C$ values of 20-yr samples back to 5220 BC, and of a mixture of intervals (single yr to up to 20 yr) prior to that.

Detailed atmospheric $\Delta^{14}C$ on a decadal scale is given in Figure 2 for the last 4500 yr (Stuiver & Becker, 1986).

For the carbon reservoir modeling, we constructed a curve with bi-decadal coverage for the entire AD 1950–7740 BC interval. The initial equilibrium conditions of the model were set at an atmospheric $\Delta^{14}C$ value of +90‰ (Stuiver *et al,* 1986). An important parameter of the box-diffusion model (see also Stuiver & Quay, 1981) is the atmospheric CO_2 concentration which is fixed at 280ppm (Neftel *et al,*1985; Stuiver, Burk & Quay, 1984). Oceanic C concentration is set at 2.31moles/m^3 (Takahashi, Broecker & Bainbridge, 1981). The biosphere is set at a constant 1900 Gigatons C (Olson, Pfuderer & Chan, 1978). The biosphere is divided into two reservoirs with residence times of 2.7 yr and 80 yr (Emanuel *et al,* 1984). The reservoir with fast turnover contains 10.6% of the total biomass, the other 89.4% (Emanuel *et al,* 1984). Gas exchange rate F is set at 19moles/m^{2}yr in order to yield a nearly 50‰ $\Delta^{14}C$ difference between the atmosphere and mixed layer in the year 1830 (the last bi-decadal midpoint without fossil fuel CO_2 influence). To generate a 40‰ difference between the atmospheric and mixed layer $\Delta^{14}C$, F has to be adjusted to 24moles/m^{2}yr.

A vertical diffusion coefficient K_z of 1.26cm^2/sec yields a deep ocean $\Delta^{14}C$ value of −190‰ in 1850, in agreement with GEOSECS measurements (Stuiver, Quay & Östlund, 1983).

MODEL RESULTS

The model input is the post-7750 BC atmospheric $\Delta^{14}C$ record, of which the post-7200 BC portion is given in the top curve of Figure 3. The $\Delta^{14}C$ values of the 550 yr preceding 7200 BC (Fig 1) were used for a proper startup of the model.

Model-derived mixed layer $\Delta^{14}C$ values (F = 19moles/m^{2}yr, K = 1.26cm^2/sec, to yield a mixed layer $\Delta^{14}C$ = −49.7‰ (R = 409 yr) at AD 1830) are given in the middle curve. Relative to the atmosphere, there is a substantial attenuation of the higher $\Delta^{14}C$ frequencies in the mixed layer. For the deep ocean (bottom curve) only a long-term trend remains.

To determine the sensitivity of the model results to the choice of F and K_z, we also generated mixed layer $\Delta^{14}C$ values with model parameters set at F = 24moles/m^{2}yr,K_z = 1.26cm^2/sec, to yield a mixed layer $\Delta^{14}C$ = −40.4‰ (R = 331 yr) at AD 1830. The difference between the F = 19 and F = 24moles/m^2 yr model outputs of mixed layer $\Delta^{14}C$ values and ^{14}C ages are given in Figure 4. Evidently the calibration curve is relatively insensitive to F because the model-calculated mixed layer ages, after normalization on the same baseline, differ by up to 16 ^{14}C years.

Eddy diffusivity is faster in the upper portion of the ocean than in the lower part (Stuiver, 1980). We compared the model-generated mixed layer ^{14}C ages for K_z values of 1.26cm^2/sec and 2.2cm^2/sec, with R set at 409 yr in AD 1830 in both cases. The faster diffusivity was accompanied by an increased exchange coefficient F of 20moles/m^{2}yr. The resulting model outputs of mixed layer ^{14}C ages differed by a fraction of a decade for the long term (millennia), as well as the shorter term (century) type oscillations. Thus, the fine structure of the model mixed layer curves is not sensitive to assumed K_z values.

Figure 5 gives the conventional ^{14}C ages of the atmosphere, mixed layer of the ocean, and the deep ocean. The differences in basic features of the atmospheric and marine calibration curves are caused by the strong attenuation in the oceans of the higher frequency $\Delta^{14}C$ perturbation. This leads to the variable R(t). With the traditional method of correcting marine ^{14}C ages one would deduct a fixed reservoir age R* (derived for one year only) from the Figure 5 results and use it for all ages. Two examples of this approach are given in Figures 6 and 7 where fixed reservoir ages of 409 yr and 1684 yr are deducted from, respectively, the mixed layer and deep ocean ^{14}C ages. The deducted reservoir ages are those calculated for the year 1830. Whereas the fixed reservoir age concept indeed gives calibration curves resembling the atmospheric one for the 4300–5000 BC interval (Fig 6), appreciable differences are found for the 200–900 BC interval (Fig 7). This is due partially to the perturbation in atmospheric $\Delta^{14}C$ between 400 and 750 BC which results in the horizontal portion of the Figure 7 atmospheric calibration curve. This perturbation is much smaller in the mixed layer, and absent in the deep ocean (Fig 7). Similarly, the lag in deep ocean response to the long-term post 5000 BC atmospheric $\Delta^{14}C$ decline results in the lower curve offset in Figure 7.

Atmospheric $\Delta^{14}C$ changes in our model are caused by production rate changes. The atmospheric $\Delta^{14}C$ changes in turn influence the oceans. A reverse scenario in which changes in ocean circulation lead to atmospheric $\Delta^{14}C$ changes is contradicted by the work of Andrée *et al* (1986a) on the ^{14}C age differences of the mixed layer and the deep ocean. These age differences were derived from the ^{14}C ages of planktonic and benthic marine organisms in two sediment cores of the South China Sea (Fig 8). As discussed by Andrée *et al* (1986a), a drastic post 6000 BP speed-up in ocean circulation is needed if the oceans would be the primary cause of the long-term change (Fig 1) in atmospheric $\Delta^{14}C$ values. For this scenario a much lower rate of ocean mixing is needed in the early Holocene which would generate ^{14}C age differences twice as large as currently found between mixed layer and deep ocean (Andrée *et al*, 1986a). As this is not the case (Fig 8), our first order assumption of constant reservoir parameters is justified. It should be noted, however, that even with a fixed mode of ocean circulation, changes of up to 200 yr are possible in the mixed layer-deep sea Holocene ^{14}C age differences (Fig 8).

The variable reservoir ages R(t) of the mixed layer and deep ocean deduced from Figure 5 are given in Figure 9A. The atmospheric $\Delta^{14}C$ lowering associated with fossil fuel combustion decreases the reservoir age of the mixed layer and deep ocean by about, respectively, 100 yr and 170 yr between AD 1850 and 1950 (Fig 9B).

RADIOCARBON AGE CALIBRATION AND ΔR DETERMINATION

The question arises how a user provided with a conventional ^{14}C age of a sample from a certain part of the ocean should use the calibration curves that are calculated for the world oceans. After proper correction for isotope fractionation (Stuiver & Polach, 1977), the conventional ^{14}C ages of marine shells are generally too old. The age anomaly (reservoir age) is 200 to 400 yr for the mixed layer of the world oceans, but may be larger in areas of upwelling (up to 1300 yr, Stuiver & Braziunas, 1985).

Our calibration curves depict the relationship between cal AD/BC (cal BP) ages and *conventional* (Stuiver & Polach, 1977) ^{14}C ages. Those ^{14}C ages are corrected for isotope fractionation, but not for any reservoir deficiency. The model mixed layer and deep ocean reservoir ages average, respectively, 373 yr and 1554 yr over the last 9000 yr. These averages result from our choice of specific model parameters and do not reflect local variations in the ocean reservoir ages.

To accommodate local effects, the model ocean can be matched with regional parts of the world ocean by assuming a parallel $\Delta^{14}C$ response, *ie*, we assume as a first approximation identical time-dependent response of the regional and world ocean to atmospheric forcing. Further refinement would be possible if each region could be modeled separately. However, we have to work at present with the above approximation.

The reader of the previous sections will have noticed the time-dependent character of the reservoir age R(t) of the mixed layer of the ocean. The reservoir age, or the conventional ^{14}C age difference between samples formed contemporaneously in the mixed layer and the atmosphere, is time-dependent because the oceanic $\Delta^{14}C$ response to atmospheric $\Delta^{14}C$ forcing differs from the atmospheric signal. However, an approximately parallel response to atmospheric forcing of a regional part of the ocean and the world ocean results in a constant difference (ΔR) in reservoir age of the two. Thus, although reservoir ages are time-dependent, ΔR, as a first approximation, is not.

The difference ΔR in reservoir age of the regional part of the ocean from which the users sample is derived, and the reservoir age of our model ocean, is determined through the use of Figure 10A. The user needs information on reservoir ages, *ie*, a ^{14}C age P should be available for a historic (year AD X) sample collected from the same reservoir from which his/her sample is derived. The user has to derive from Fig 10A the model mixed layer (or deep ocean) ^{14}C age Q for year AD X. The correction factor to be used for the sample ^{14}C age in the calibration Figures 11 and 12 is then $\Delta R = P - Q$.

In case the user lacks information on ^{14}C ages of historic samples he/she can assume the sample comes from an environment similar to the model world ocean. The Figure 11 and 12 calibration curves (with $\Delta R = 0$) can then be used directly.

Our calculations neglect hemispheric reservoir differences that cause ^{14}C ages of atmospheric samples of the Southern Hemisphere to be ca 30 years older than those of the Northern Hemisphere. Hemispheric differences will be taken into account in a model currently being developed by one of us (T Braziunas).

Suggested ΔR values for various oceanic regions are plotted in Figure 10B. These weighted mean ΔR values were derived from ^{14}C ages listed in Table 1, which also gives the sample groupings from which the average ΔR values were derived. Except for a few instances, Table 1 contains only shell sample dates.

The standard deviations given with ΔR in Table 1 were derived from the errors reported with the ^{14}C ages. The ^{14}C age groupings also can be viewed as a data set from which the standard deviation ("scatter" sigma) in the unweighted mean can be calculated. These "scatter" sigmas in the unweighted mean are given in Table 1.

The largest of each set of sigmas was used for the ± value plotted in Figure 10B. In view of the much debated under-reporting of ^{14}C age errors, it was gratifying to see that the scatter sigma was, on average, only 1.1 times the ^{14}C age sigma. From this we conclude 1) the additional uncertainty in ΔR introduced by non-uniform ^{14}C content of the regional ocean reservoirs is small, and 2) the age errors given for the Table 1 shell samples are realistic estimates of the measurement precision.

The uncertainty in the age conversion process depends on the extent to which a particular sample's environment resembles the average model world ocean, and on the degree to which the model simulates the reality. It is not possible to give these uncertainties as standard deviations, and the calibration curves therefore lack an uncertainty band.

When converting a conventional ^{14}C age into cal AD/BC (or cal BP) age, the standard deviation in the sample age determination σ_s should be taken into account. There will be an additional error in either the determined or the assumed reservoir age difference ΔR. As noted, $\Delta R = P - Q$ where P is the conventional ^{14}C age of an historic sample, and Q the model-calculated conventional ^{14}C age of a sample of the same historic age. The ΔR error (σ_R) depends on the error in P, as well as Q. We do not have a standard error for the model-calculated Q value. Only a lower limit can be given for σ_R by substituting the error in the ^{14}C age determination P. This error is listed in Table 1 as a "minimum estimate" for σ_R.

The σ_R should be combined with σ_s according to $\sigma_{total} = \sqrt{\sigma_s^2 + \sigma_R^2}$. The

(^{14}C age − ΔR) ± σ_{total}, after conversion, determines a minimum range in calibrated ages.

Marine and "atmospheric" samples with identical ^{14}C ages and standard deviations will differ in calibrated age, as well as in the range in calibrated ages. The cal range will usually be larger for the marine sample due to the incorporation of the standard deviation σ_R in the reservoir age difference ΔR. The issue of multiple intercepts, however, is much less important for marine samples because the calibration curves (Figs 11, 12) are much less wiggley than the corresponding atmospheric ones (eg, Stuiver & Pearson, 1986).

ACKNOWLEDGMENTS

^{14}C research of the Quaternary Isotope Laboratory is supported through National Science Foundation grant ATM-8318665 of the Climate Dynamics Program and EAR-8115994 of the Environmental Geosciences Program. The work of the Belfast laboratory was supported through a SERC grant to the Queens University. P D Quay generously provided the basic carbon reservoir computer model from which, after modifications, the calculations were made.

REFERENCES

Andrée, M, Oeschger, H, Broecker, W S, Beavean, N, Klas, M, Mix, A, Bonani, G, Hofmann, H J, Suter, M, Woelfli, W and Peng, T H, 1986a, Limits on the ventilation rate for the deep ocean over the last 12,000 years: Climate Dynamics, v 1, in press.

Andrée, M, Oeschger, H, Siegenthaler, U, Riesen, T, Moell, M, Amman, B and Tobolski, K, 1986b, ^{14}C dating by AMS of plant macrofossils in lake sediment, *in* Stuiver, M and Kra, R S, eds, Internatl ^{14}C conf, 12th, Proc: Radiocarbon, v 28, no. 2A, p 411–416.

Berger, R, Taylor, R E and Libby, W F, 1966, Radiocarbon content of marine shells from the California and Mexican west coast: Science, v 153, p 864–866.

Broecker, W S and Olson, E A, 1959, Lamont radiocarbon measurements VI: Am Jour Sci Radiocarbon Supp, v 1, p 111–132.

Broecker, W S and Olson, E A, 1961, Lamont radiocarbon measurements VII: Radiocarbon, v 3, p 176–204.

Druffel, E M and Linick, T W, 1978, Radiocarbon in annual coral rings of Florida: Geophys Research Letters, v 5, p 913–916.

Emanuel, W R, Killough, G G, Post, W M and Shugart, H H, 1984, Modeling terrestrial ecosystems in the global carbon cycle with shifts in carbon storage capacity by land-use change: Ecology, v 65, no. 3, p 970–983.

Gillespie, R and Polach, H A, 1979, The suitability of marine shells for radiocarbon dating of Australian prehistory, *in* Berger, R and Suess, HE, eds, Radiocarbon dating, Internatl ^{14}C conf, 9th, Proc: Berkeley, Univ California Press, p 404–421.

Hakansson, S, 1969, University of Lund radiocarbon dates II: Radiocarbon, v 11, no. 2, p 430–450.

——————1970, University of Lund radiocarbon dates III: Radiocarbon, v 12, no. 2, p 534–552.

—————— 1973, University of Lund radiocarbon dates VI: Radiocarbon, v 15, no. 3, p 493–513.

Kromer, B, Rhein, M, Bruns, M, Schoch-Fischer, H, Münnich, KO, Stuiver, M and Becker, B, 1986, Radiocarbon calibration data for the 6th to the 8th millenium BC, *in* Stuiver, M and Kra, R S, eds, Internatl ^{14}C conf, 12th, Proc: Radiocarbon, this issue.

Linick, T W, Long, A, Damon, P E and Ferguson, C W, 1986, High-precision radiocarbon dating of bristlecone pine from 6550 to 5350 BC, *in* Stuiver, M and Kra, R S, eds, Internatl ^{14}C conf, 12th, Proc: Radiocarbon, this issue.

Linick, T W, Suess, H E and Becker, B, 1985, La Jolla measurements of radiocarbon in South German Oak tree-ring chronologies: Radiocarbon, v 27, no. 1, p 20–32.

Mangerud, J, 1972, Radiocarbon dating of marine shells, including a discussion of apparent age of recent shells from Norway: Boreas, v 1, p 143–172.

Mangerud, J and Gulliksen, S, 1975, Apparent radiocarbon ages of Recent marine shells from Norway, Spitsbergen, and Arctic Canada: Quaternary Research, v 5, p 263–273.

Neftel, A, Moore, E, Oeschger, H and Stauffer, B, 1985, Evidence from polar ice cores for the increase in atmospheric CO_2 in the past two centuries: Nature, v 315, p 45–47.

Oeschger, H, Siegenthaler, U, Schotterer, U and Gugelmann, A, 1975, A box diffusion model to study the carbon dioxide exchange in nature: Tellus, v 27, p 168–192.

Olson, J S, Pfuderer, H A and Chan, Y H, 1978, Changes in the global carbon cycle and the biosphere: Environmental Sci Div, Oak Ridge Natl Lab Pub No. 1050.

Olsson, I U, 1960, Uppsala natural radiocarbon measurements II: Am Jour Sci Radiocarbon Supp, v 2, p 112–128.

—————— 1980, Content of ^{14}C in marine mammals from northern Europe, *in* Stuiver, M and Kra, R S, eds, Internatl ^{14}C conf, 10th, Proc: Radiocarbon, v 22, no. 3, p 662–675.

Olsson, I U, El-Gammal, S and Goksu, Y, 1969, Uppsala natural radiocarbon measurements IX: Radiocarbon, v 11, no. 2, p 515–544.

Pearson, G W, Pilcher, J R, Baillie, M G L, Corbett, D M and Qua, F, 1986, High-precision ^{14}C measurement of Irish Oaks to show the natural ^{14}C variations from 5210 BC to AD 1840, *in* Stuiver, M and Kra, R S, eds, Internatl ^{14}C conf, 12th, Proc: Radiocarbon, this issue.

Pearson, G W and Stuiver, M, 1986, High-precision calibration of the radiocarbon time scale 500–2500 BC, *in* Stuiver, M and Kra, R S, eds, Internatl ^{14}C conf, 12th, Proc: Radiocarbon, this issue.

Rafter, T A, Jansen, H S, Lockerbie, L and Trotter, M M, 1972, New Zealand radiocarbon reference standards, *in* Rafter, T A and Grant-Taylor, T, eds, Internatl conf on ^{14}C dating, 8th, Proc: Wellington, Royal Soc New Zealand, v 2, p H29–H79.

Robinson, S W and Thompson, G, 1981, Radiocarbon corrections for marine shell dates with application to southern Pacific Northwest Coast prehistory: Syesis, v 14, p 45–57.

Sternberg, R S and Damon, P E, 1983, Atmospheric radiocarbon: implications for the geomagnetic dipole moment, *in* Stuiver, M and Kra, R S, eds, Internatl ^{14}C conf, 11th, Proc: Radiocarbon, v 25, no. 2, p 239–248.

Stuiver, M, 1980, ^{14}C distribution in the Atlantic Ocean: Jour Geophys Research, v 85, p 2711–2718.

Stuiver, M and Becker, B, 1986, A decadal high-precision calibration curve, *in* Stuiver, M and Kra, R S, eds, Internatl ^{14}C conf, 12th, Proc: Radiocarbon, this issue.

Stuiver, M and Braziunas, T F, 1985, Compilation of isotopic dates from Antarctica: Radiocarbon, v 27, no. 2A, p 117–304.

Stuiver, M and Pearson, G W, 1986, High-precision calibration of the radiocarbon time scale AD 1950–500 BC, *in* Stuiver, M and Kra, R S, eds, Internatl ^{14}C conf, 12th, Proc: Radiocarbon, this issue.

Stuiver, M and Polach, H A, 1977, Discussion: Reporting of ^{14}C data: Radiocarbon, v 19, no. 3, p 355–363.

Stuiver, M and Quay, PD, 1980, Changes in atmospheric carbon-14 attributed to a variable sun: Science, v 207, p 11–19.

—————— 1981, Atmospheric ^{14}C changes resulting from fossil fuel CO_2 release and cosmic ray flux variability: Earth Planetary Sci Letters, v 53, p 349–362.

Stuiver, M, Burk, R L and Quay, P D, 1984, ^{13}C/^{12}C ratios in tree rings and the transfer of biospheric carbon to the atmosphere: Jour Geophys Research, v 89, p 11731–11748.

Stuiver, M, Denton, G H, Hughes, T J and Fastook, J L, 1981, History of last glaciation: A working hypothesis, *in* Denton, G H and Hughes, T J, eds, The last great ice sheets: New York, John Wiley & Sons, p 319–440.

Stuiver, M, Kromer, B, Becker, H and Ferguson, C W, 1986, Radiocarbon age calibration back to 13,300 yr BP and the ^{14}C age matching of the German Oak and U S Bristlecone Pine chronologies, *in* Stuiver, M and Kra, R S, eds, Internatl ^{14}C conf, 12th, Proc: Radiocarbon, this issue.

Stuiver, M, Quay, PD and Östlund, H G, 1983, Abyssal water carbon-14 distribution and the age of the world oceans: Science, v 219, p 849–851.

Takahashi, T, Broecker, W S and Bainbridge, A E, 1981, The alkalinity and total carbon dioxide concentration in the world oceans, *in* Bolin, B, ed, Carbon cycle modelling: SCOPE 16: New York, John Wiley & Sons, p 271–286.

Taylor, R E and Berger, R, 1967, Radiocarbon content of marine shells from the Pacific coasts of Central and South America: Science, v 158, p 1180–1182.

Washburn, A L and Stuiver, M, 1962, Radiocarbon-dated postglacial delevelling in north-east Greenland and its implications: Arctic, v 15, p 66–73.

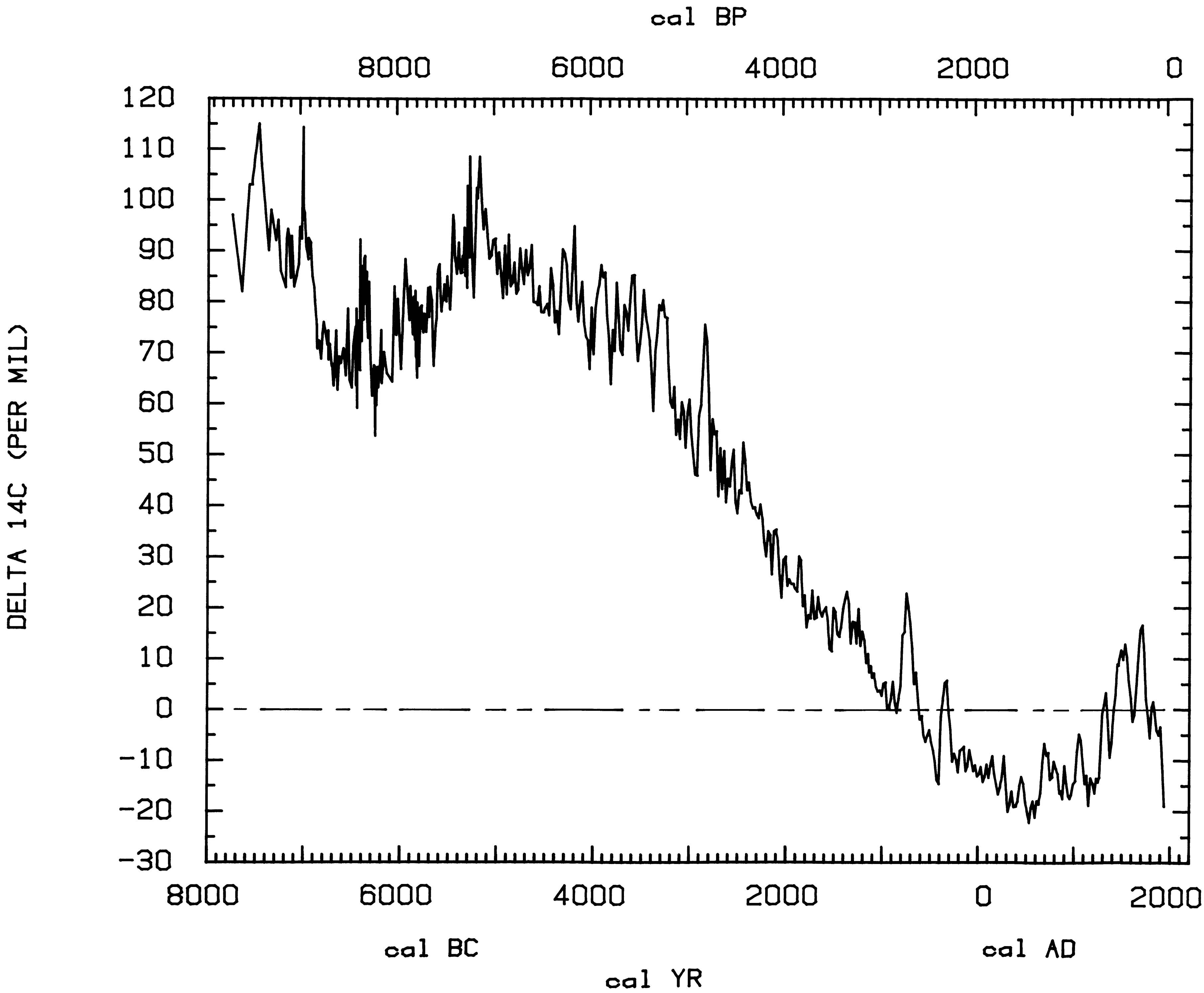

Fig 1. Atmospheric $\Delta^{14}C$ *vs* age. Compiled from data sources given in the text.

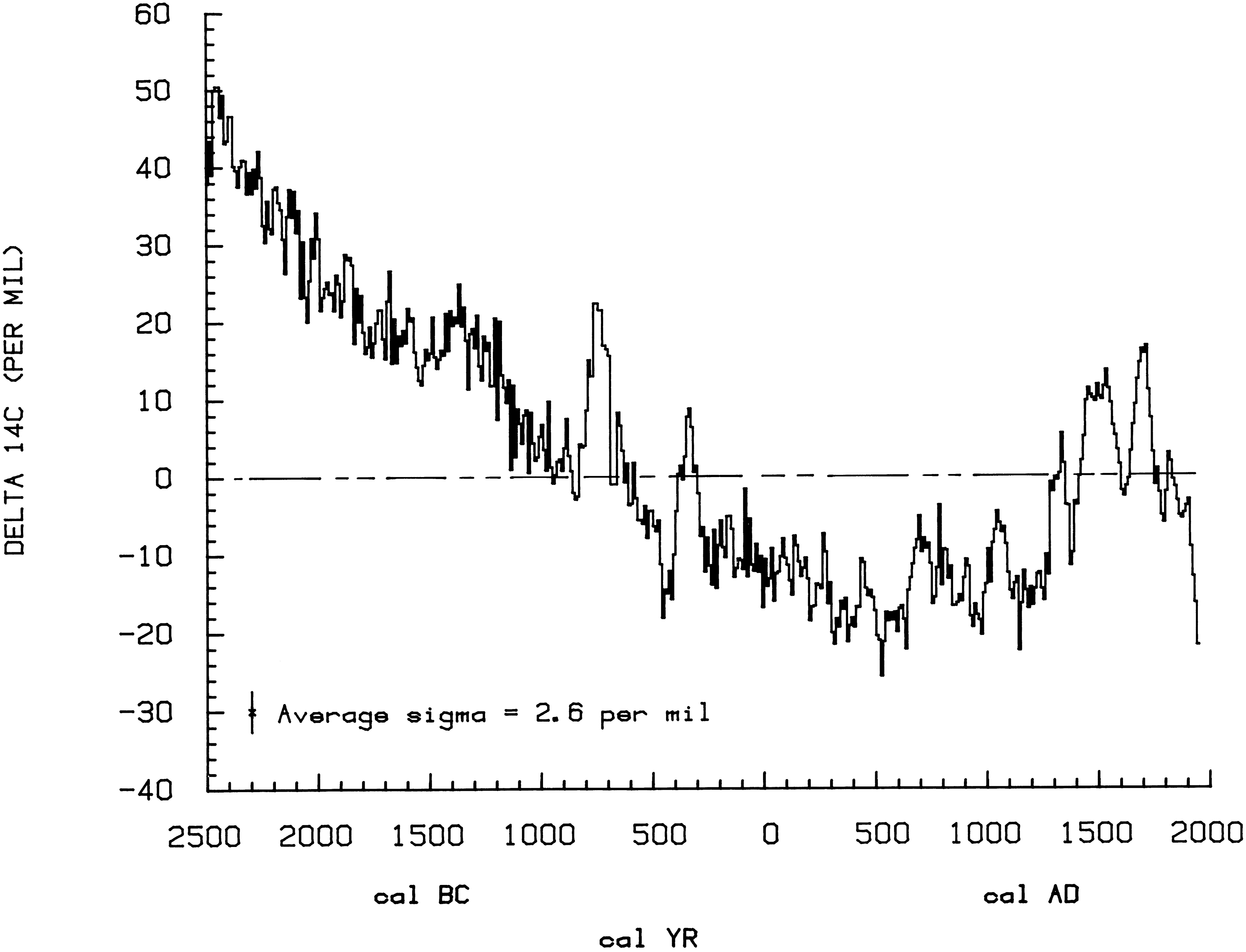

Fig 2. Atmospheric $\Delta^{14}C$ of the past 4½ millennia for each decade (Stuiver & Becker, 1986). The average standard deviation of the decadal measurements is 2.6‰.

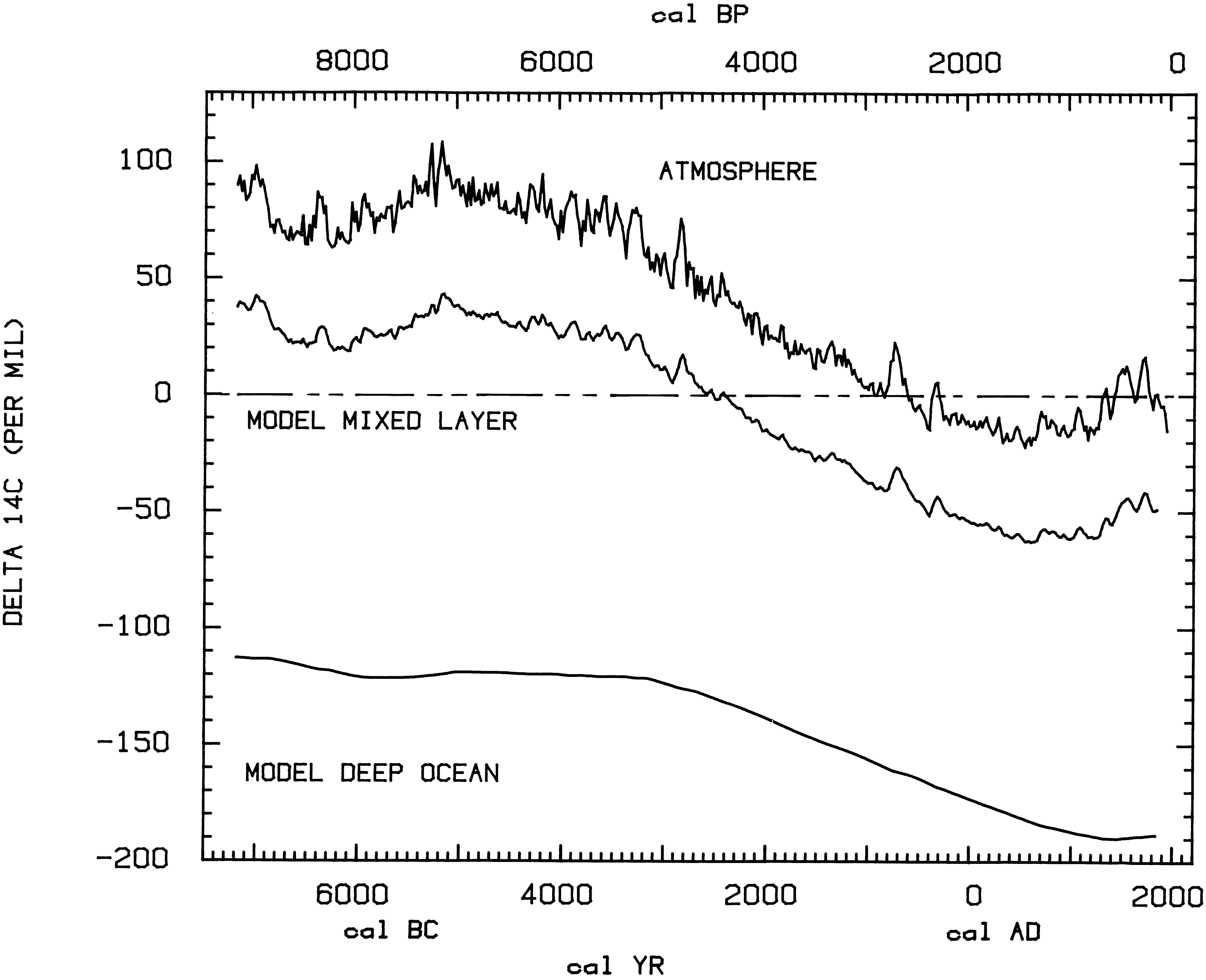

Fig 3. Atmospheric $\Delta^{14}C$ (bi-decadal values) as used for the model calculations and calculated mixed layer and deep ocean $\Delta^{14}C$ values.

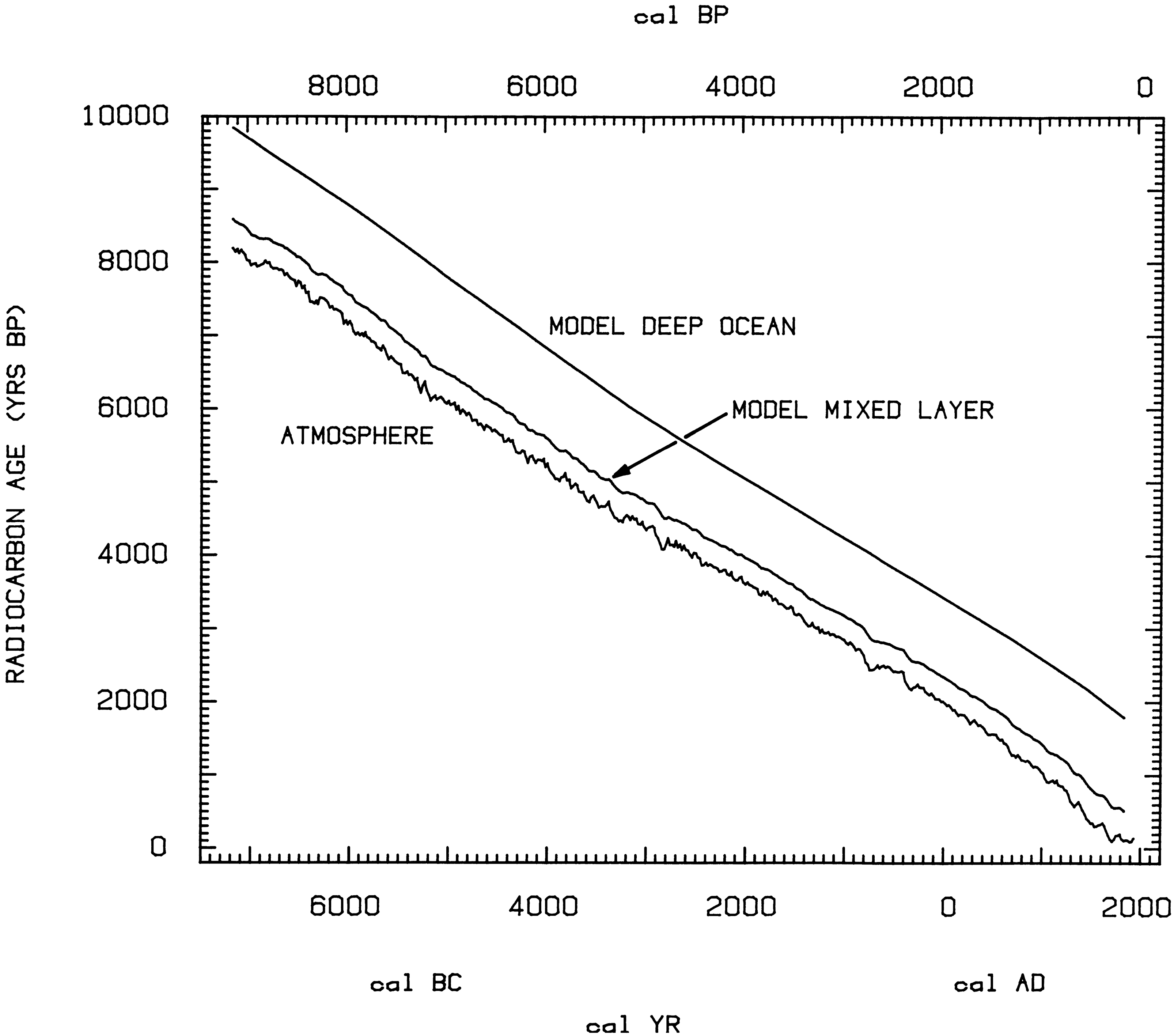

Fig 5. ^{14}C ages of the atmosphere (bi-decadal values) and calculated conventional ^{14}C ages of the mixed layer and deep ocean.

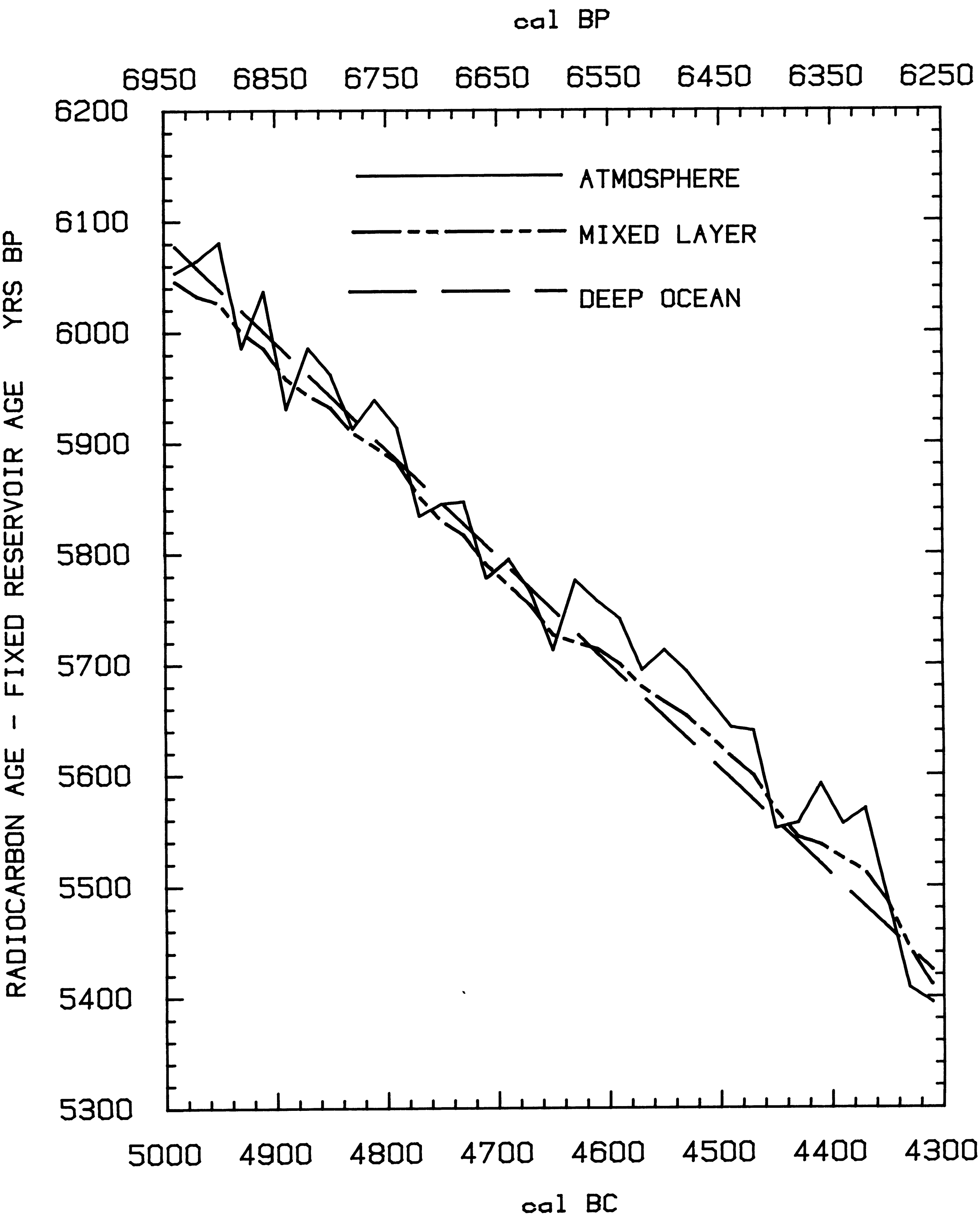

Fig 6. ^{14}C ages of "atmospheric" samples compared to reservoir corrected mixed layer and deep ocean ^{14}C ages for the 4300–5000 BC interval. The fixed reservoir correction was 409 yr and 1684 yr for, respectively, the mixed layer and the deep ocean.

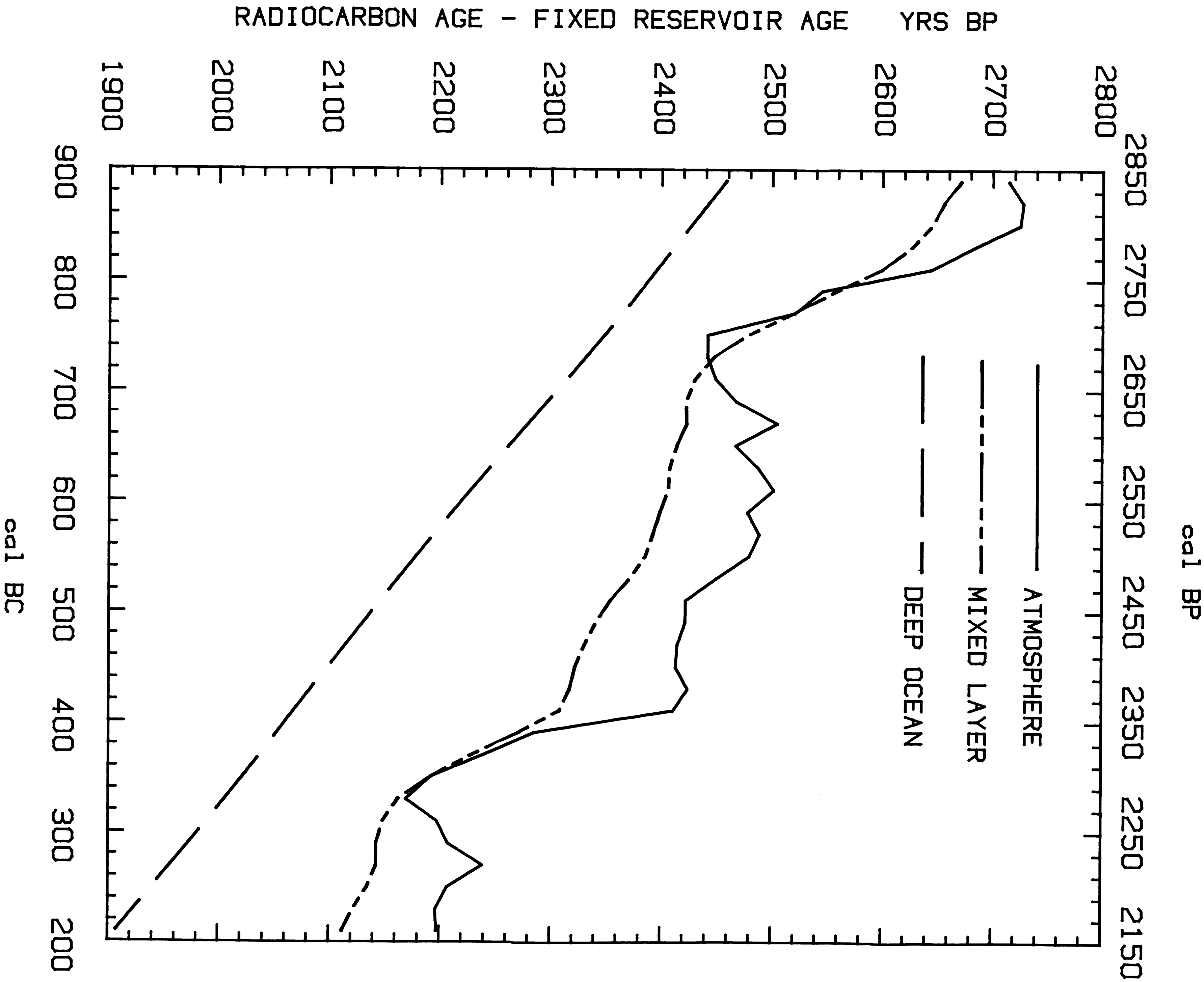

Fig 7. Similar to Figure 6 for the years 200–900 BC.

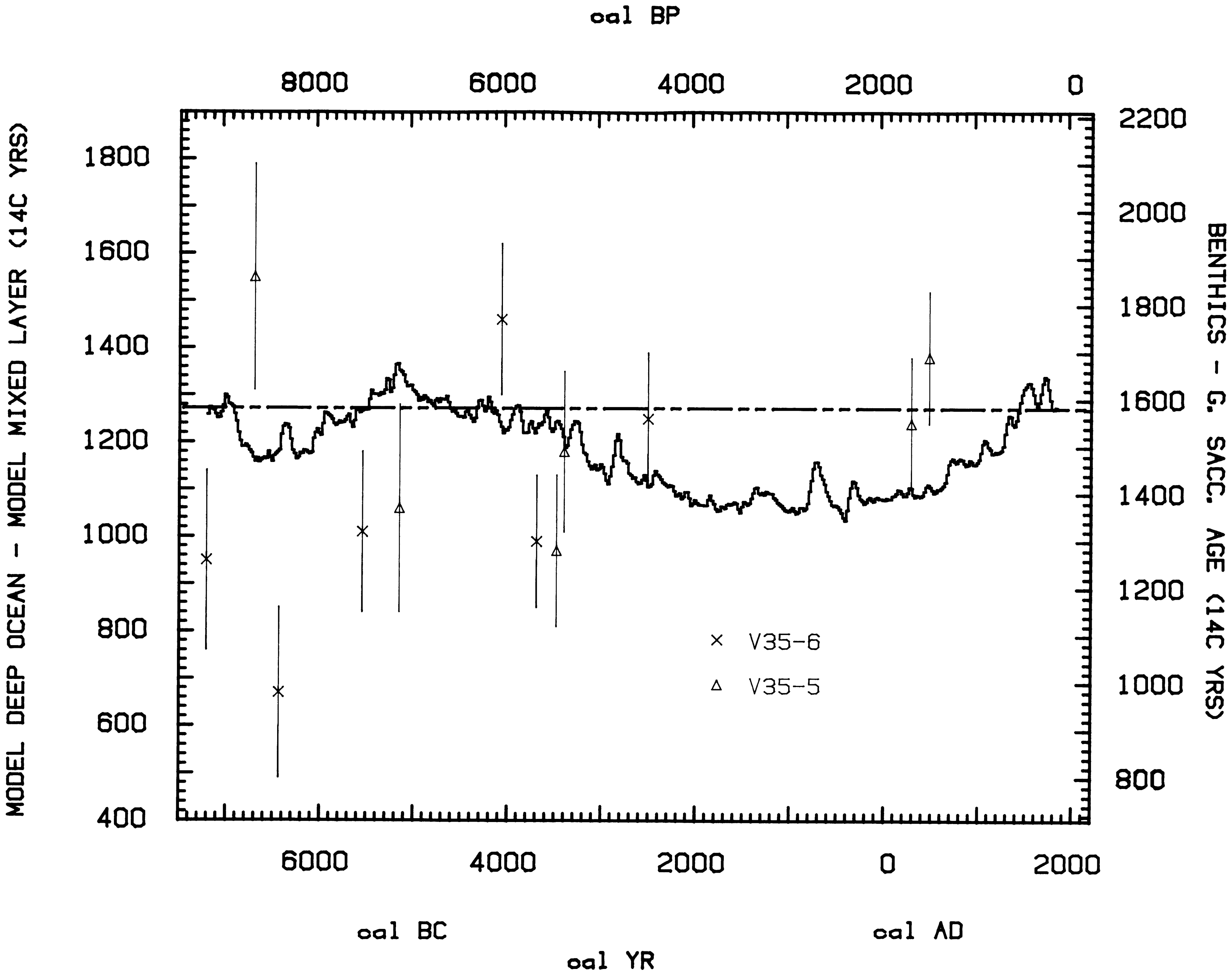

Fig 8. The calculated deep ocean-mixed layer ^{14}C age differences compared to benthic-planktonic differences measured by Andrée *et al* (1986a) for the South China Sea. The deep water in the China Sea is more ^{14}C-deficient than our model ocean, causing a shift between the ^{14}C time scales of 1585 (latest pre-anthropogenic age difference in Andrée *et al*) minus 1275 ^{14}C years (model AD 1830 value), both indicated by the dotted line.

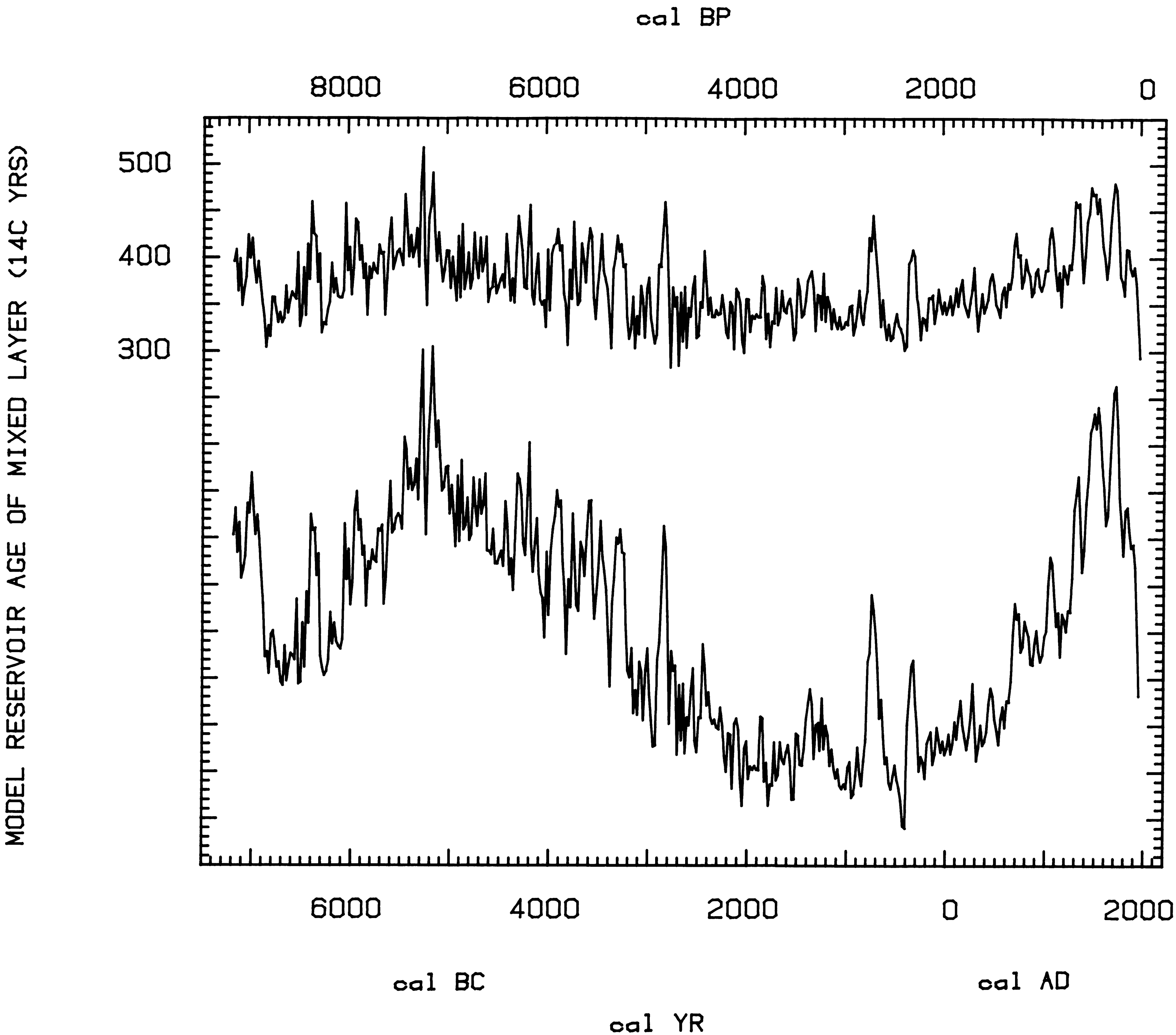

Fig 9. The changing pattern of model-calculated reservoir ages R(t) of the mixed layer (top curve) and the deep ocean (bottom curve).

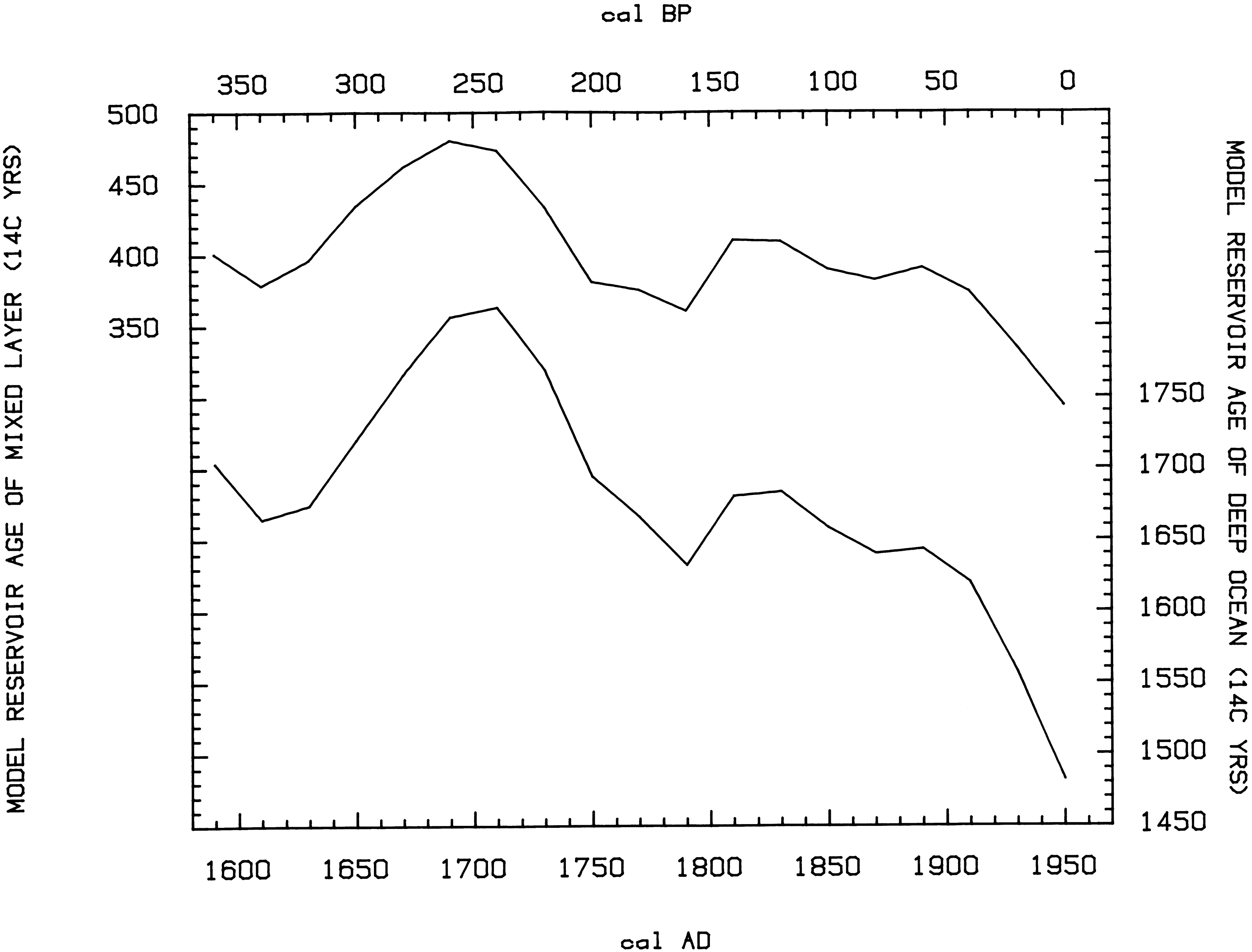

Fig 9B. Model calculated reservoir age for the mixed layer of the ocean (upper curve) and the deep ocean (lower curve).

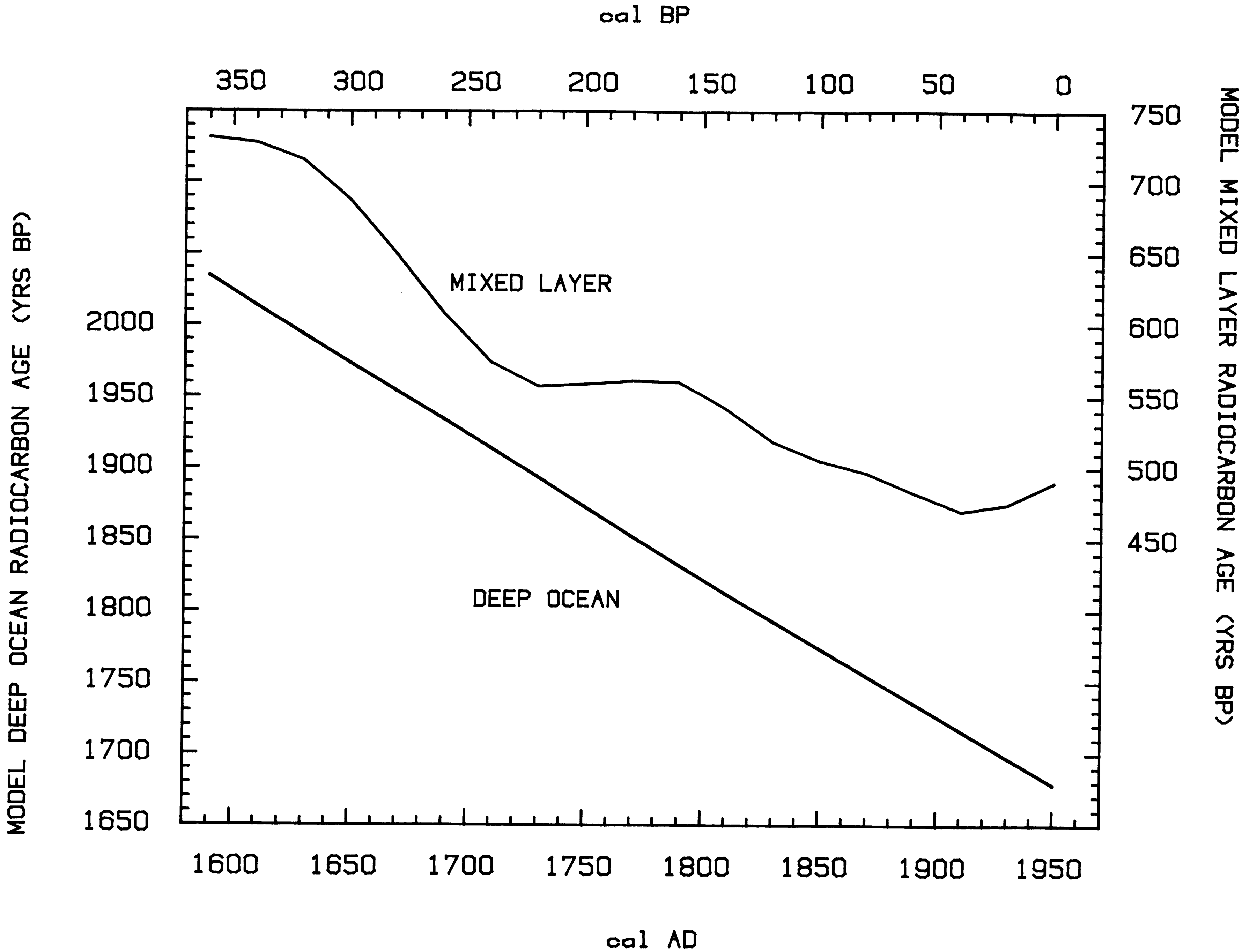

Fig 10A. Model-calculated conventional ^{14}C ages of the mixed layer and deep ocean for the AD 1600–1950 interval.

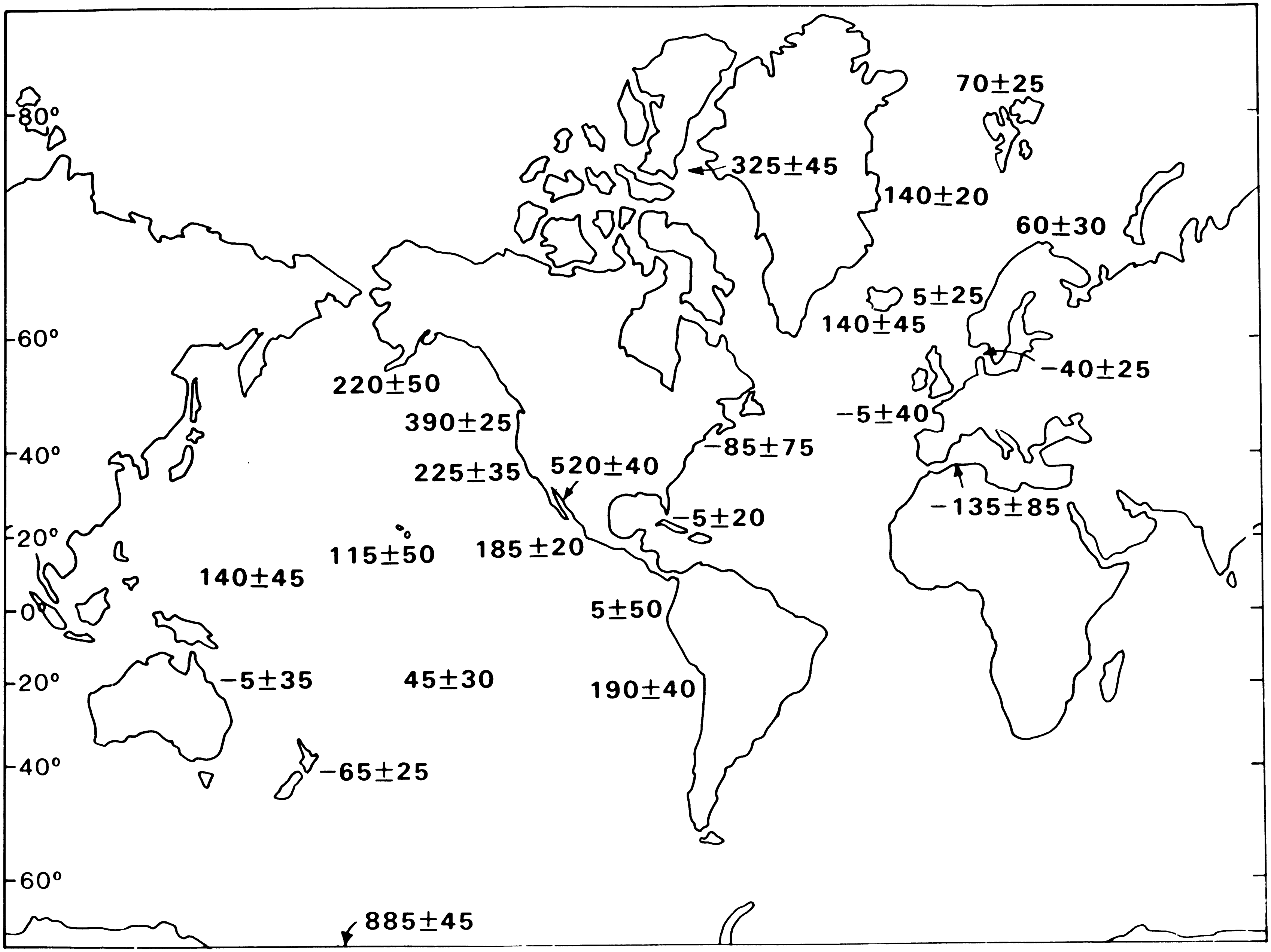

Fig 10B. Coastal region ΔR values in ^{14}C yr as derived mostly from shell dates. The ± values are minimum standard deviations based on the scatter of the data, or the measurement precision, whichever is larger (see Table 1 for details).

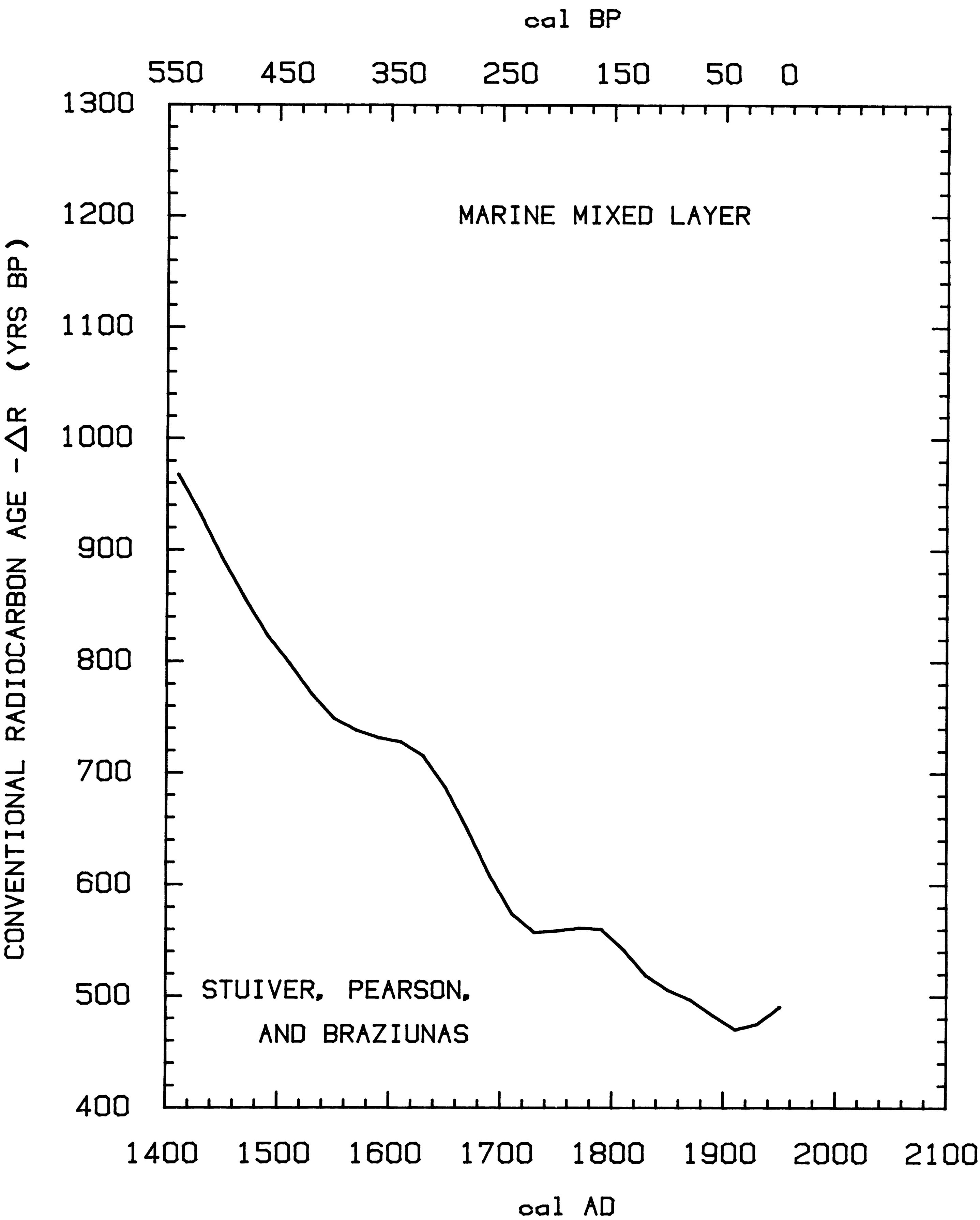

Fig 11. Mixed layer conventional ^{14}C ages *vs* cal AD/BC (cal BP) ages. The value to be substituted for ΔR is discussed in the text.

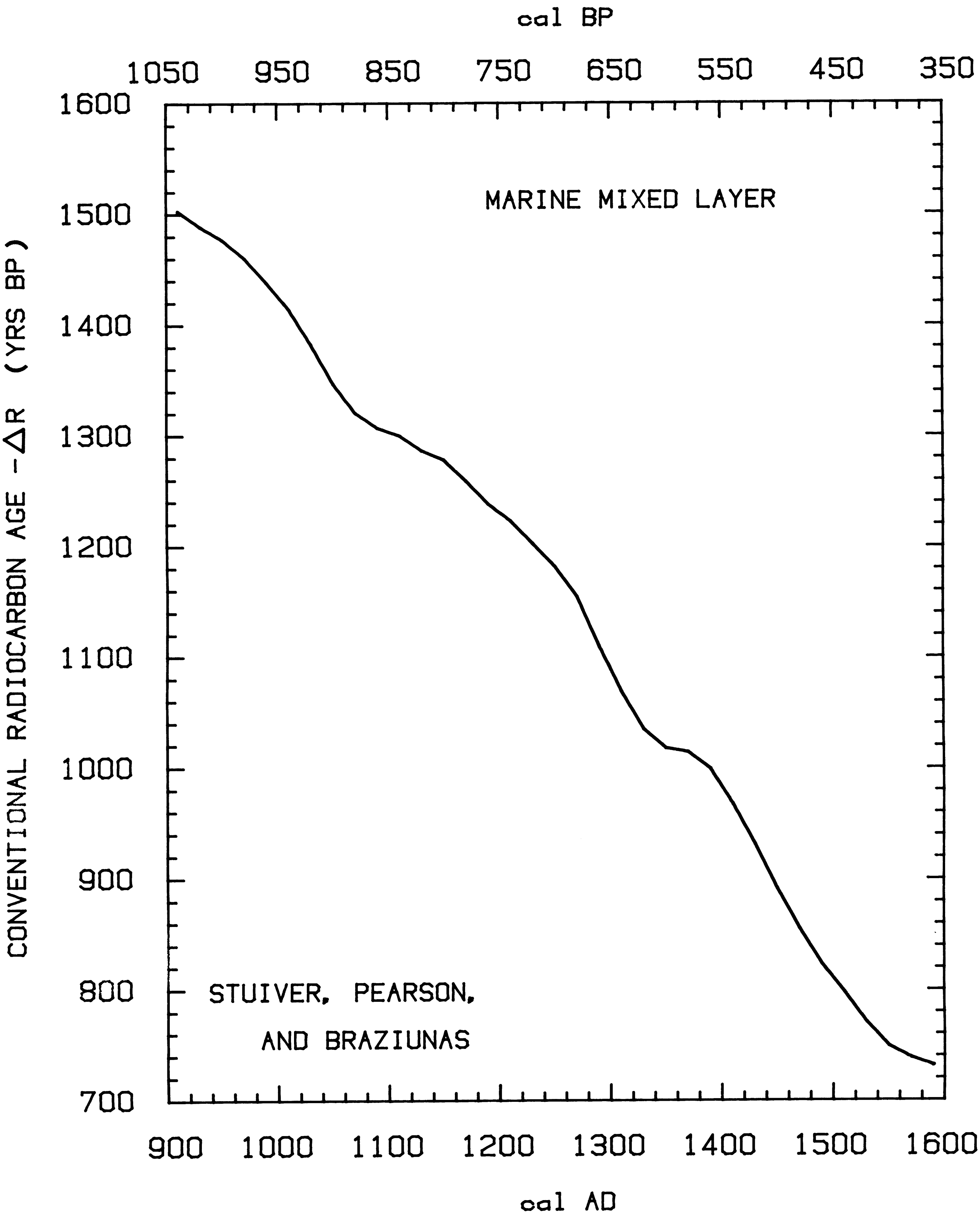
cal BP
1050
950
850
750
650
550
450
350
MARINE MIXED LAYER
CONVENTIONAL RADIOCARBON AGE -ΔR (YRS BP)
1600
1500
1400
1300
1200
1100
1000
900
800
700
STUIVER, PEARSON,
AND BRAZIUNAS
900
1000
1100
1200
1300
1400
1500
1600
cal AD

Fig 11B

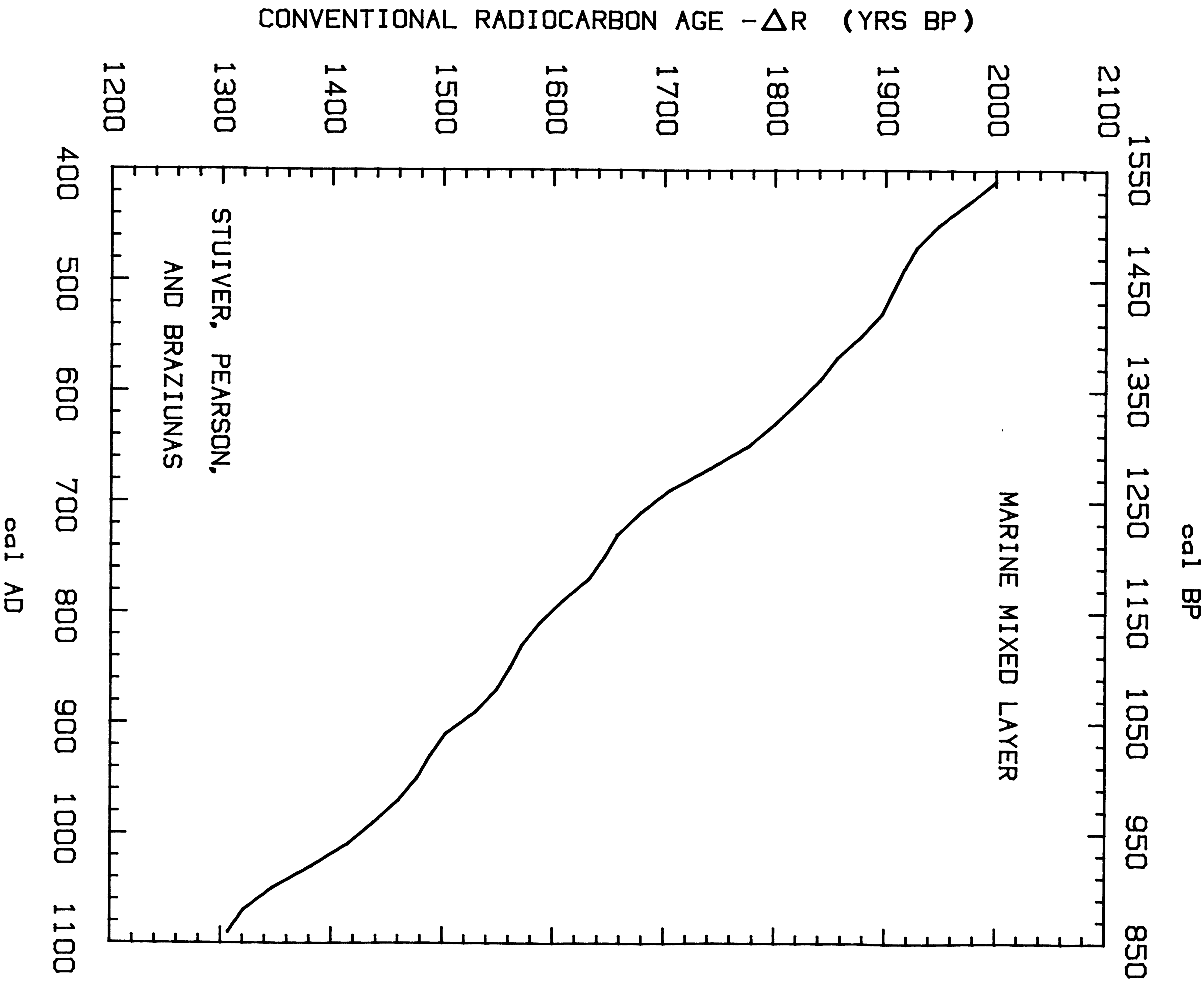
CONVENTIONAL RADIOCARBON AGE $-\Delta R$ (YRS BP)
1200
1300
1400
1500
1600
1700
1800
1900
2000
2100
cal BP
1550
1450
1350
1250
1150
1050
950
850
cal AD
400
500
600
700
800
900
1000
1100
MARINE MIXED LAYER
STUIVER, PEARSON,
AND BRAZIUNAS

Fig 11C

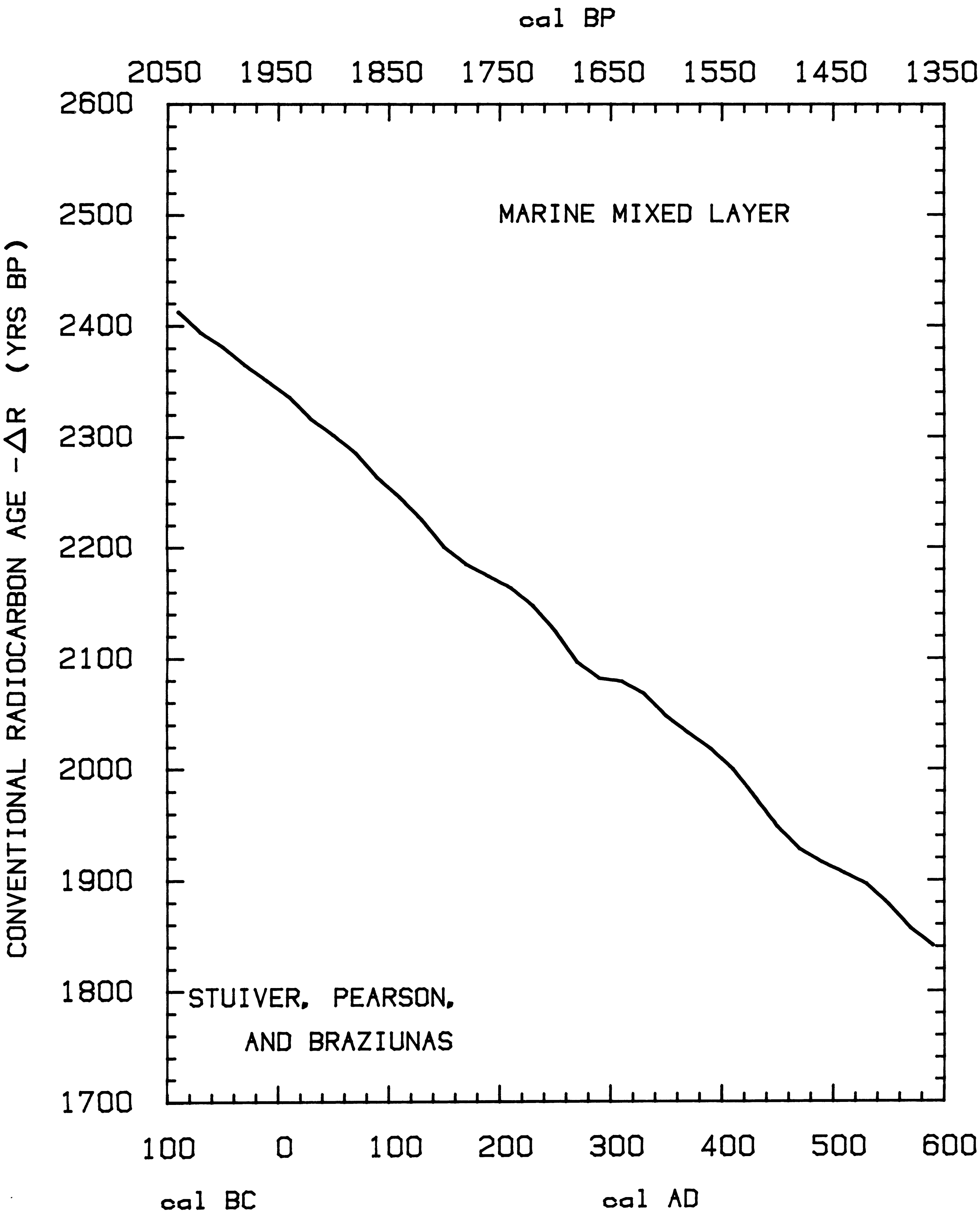
cal BP
2050 1950 1850 1750 1650 1550 1450 1350
CONVENTIONAL RADIOCARBON AGE -ΔR (YRS BP)
2600 2500 2400 2300 2200 2100 2000 1900 1800 1700
MARINE MIXED LAYER
STUIVER, PEARSON,
AND BRAZIUNAS
100 0 100 200 300 400 500 600
cal BC
cal AD

Fig 11D

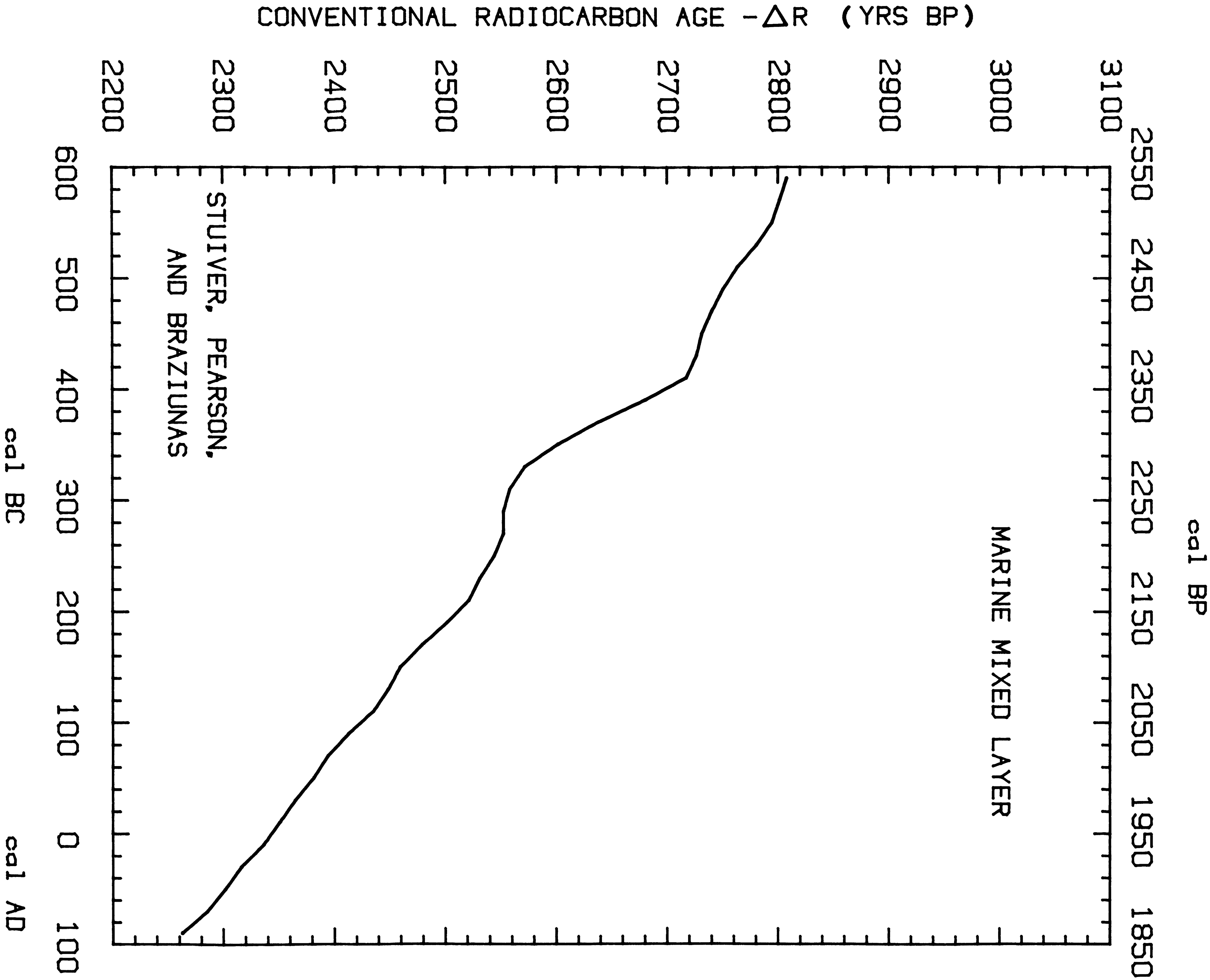
CONVENTIONAL RADIOCARBON AGE -ΔR (YRS BP)
2200
2300
2400
2500
2600
2700
2800
2900
3000
3100
cal BP
2550
2450
2350
2250
2150
2050
1950
1850
MARINE MIXED LAYER
STUIVER, PEARSON, AND BRAZIUNAS
600
500
400
300
200
100
0
100
cal BC
cal AD

Fig 11E

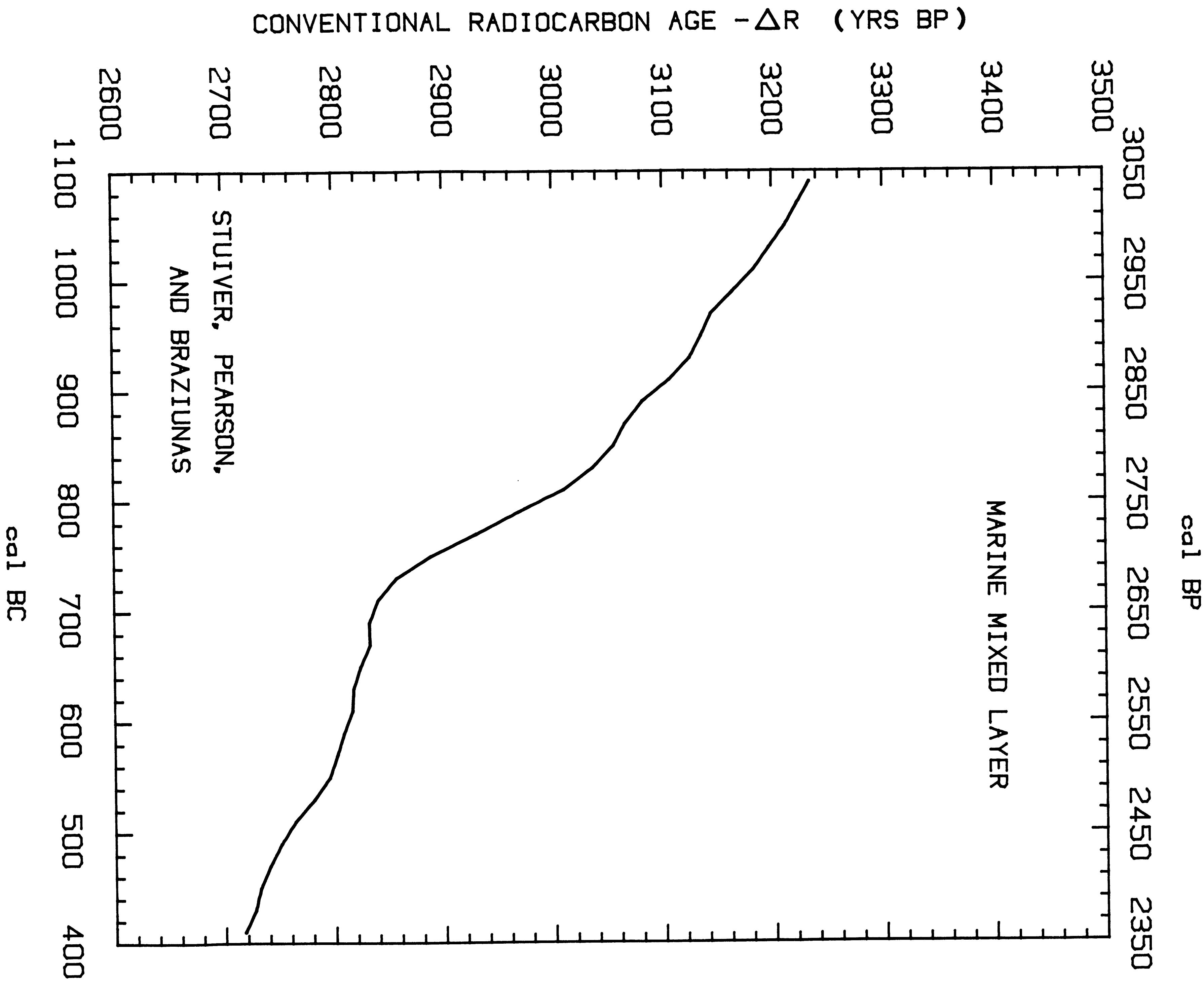
CONVENTIONAL RADIOCARBON AGE -ΔR (YRS BP)
2600
2700
2800
2900
3000
3100
3200
3300
3400
3500
cal BP
3050
2950
2850
2750
2650
2550
2450
2350
MARINE MIXED LAYER
STUIVER, PEARSON, AND BRAZIUNAS
1100
1000
900
800
700
600
500
400
cal BC

Fig 11F

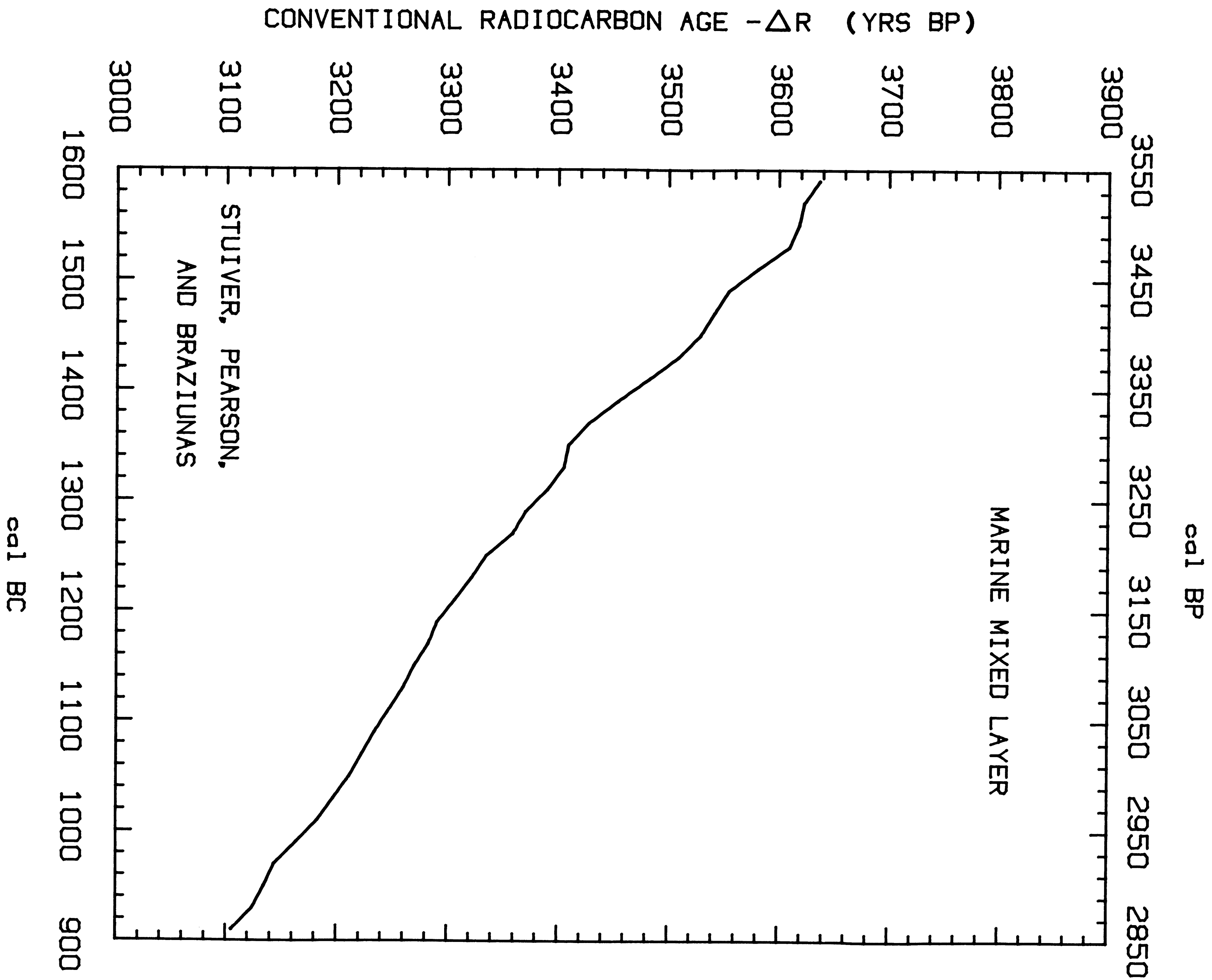
CONVENTIONAL RADIOCARBON AGE -ΔR (YRS BP)
3000
3100
3200
3300
3400
3500
3600
3700
3800
3900
cal BP
3550
3450
3350
3250
3150
3050
2950
2850
cal BC
1600
1500
1400
1300
1200
1100
1000
900
MARINE MIXED LAYER
STUIVER, PEARSON,
AND BRAZIUNAS

Fig 11G

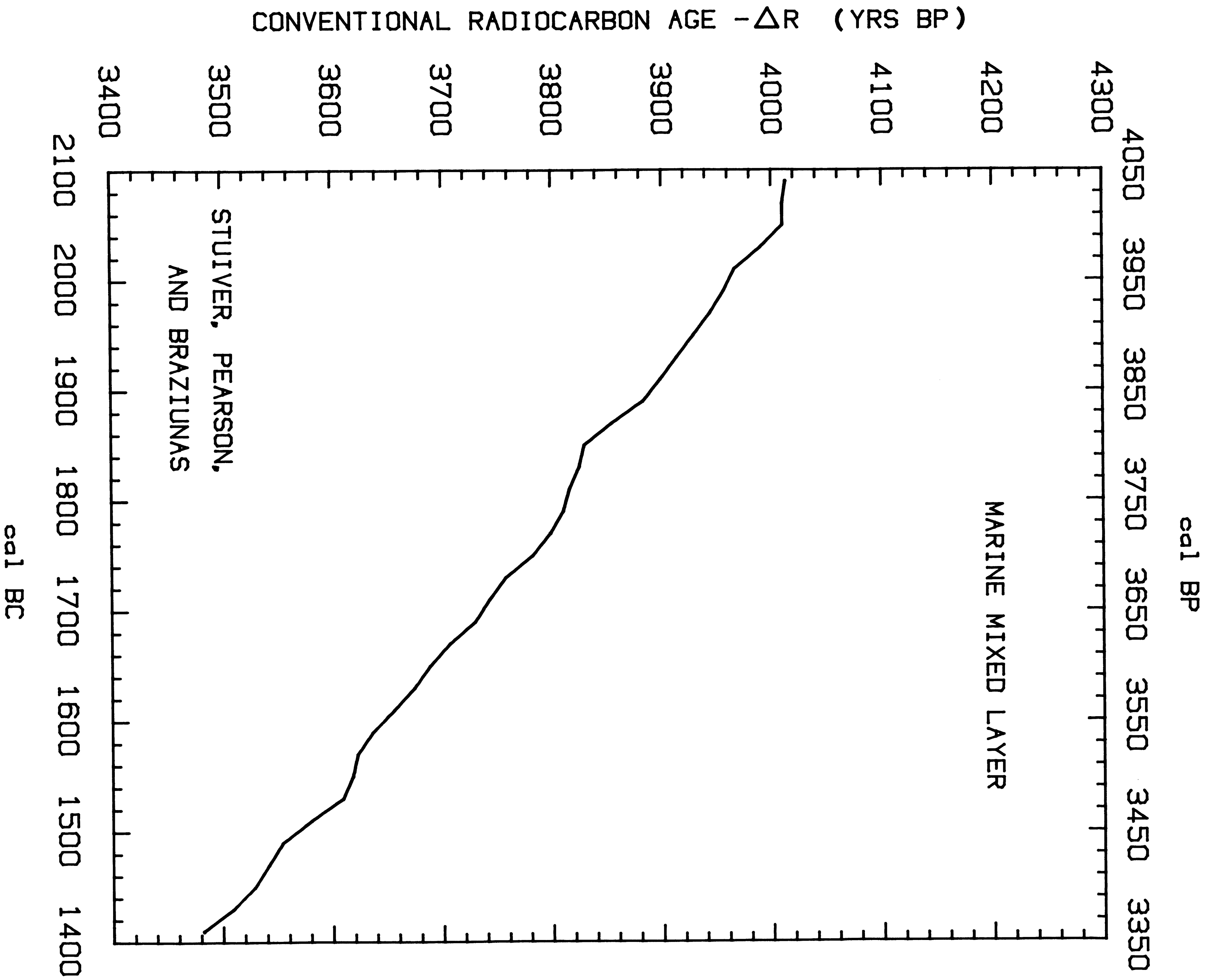
CONVENTIONAL RADIOCARBON AGE -ΔR (YRS BP)
3400
3500
3600
3700
3800
3900
4000
4100
4200
4300
cal BP
4050
3950
3850
3750
3650
3550
3450
3350
cal BC
2100
2000
1900
1800
1700
1600
1500
1400
MARINE MIXED LAYER
STUIVER, PEARSON,
AND BRAZIUNAS

Fig 11H

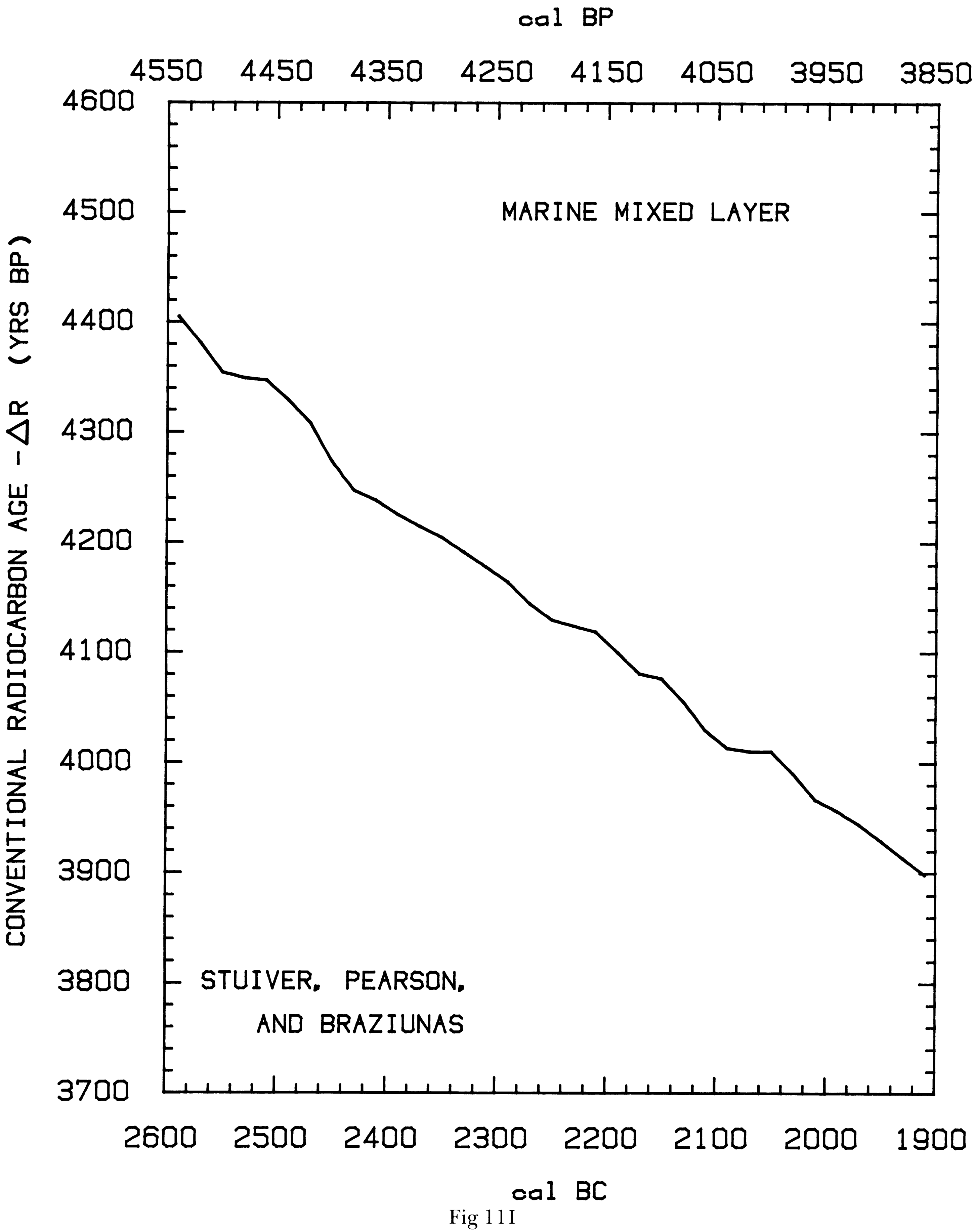
cal BP
4550
4450
4350
4250
4150
4050
3950
3850
MARINE MIXED LAYER
CONVENTIONAL RADIOCARBON AGE -ΔR (YRS BP)
4600
4500
4400
4300
4200
4100
4000
3900
3800
3700
STUIVER, PEARSON,
AND BRAZIUNAS
2600
2500
2400
2300
2200
2100
2000
1900
cal BC

Fig 11I

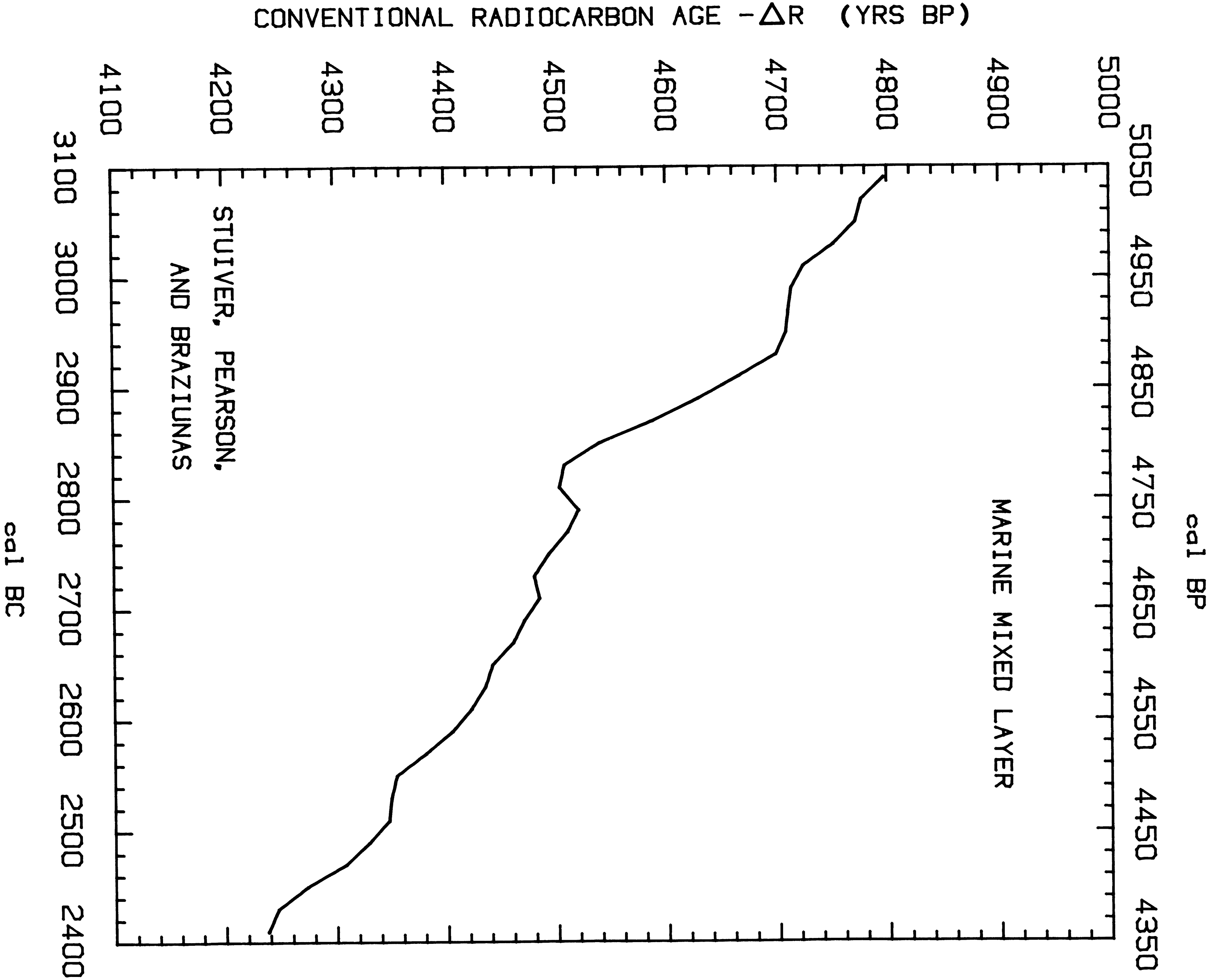

CONVENTIONAL RADIOCARBON AGE −ΔR (YRS BP)
5000
4900
4800
4700
4600
4500
4400
4300
4200
4100
cal BP
5050
4950
4850
4750
4650
4550
4450
4350
cal BC
3100
3000
2900
2800
2700
2600
2500
2400
MARINE MIXED LAYER
STUIVER, PEARSON, AND BRAZIUNAS

Fig 11J

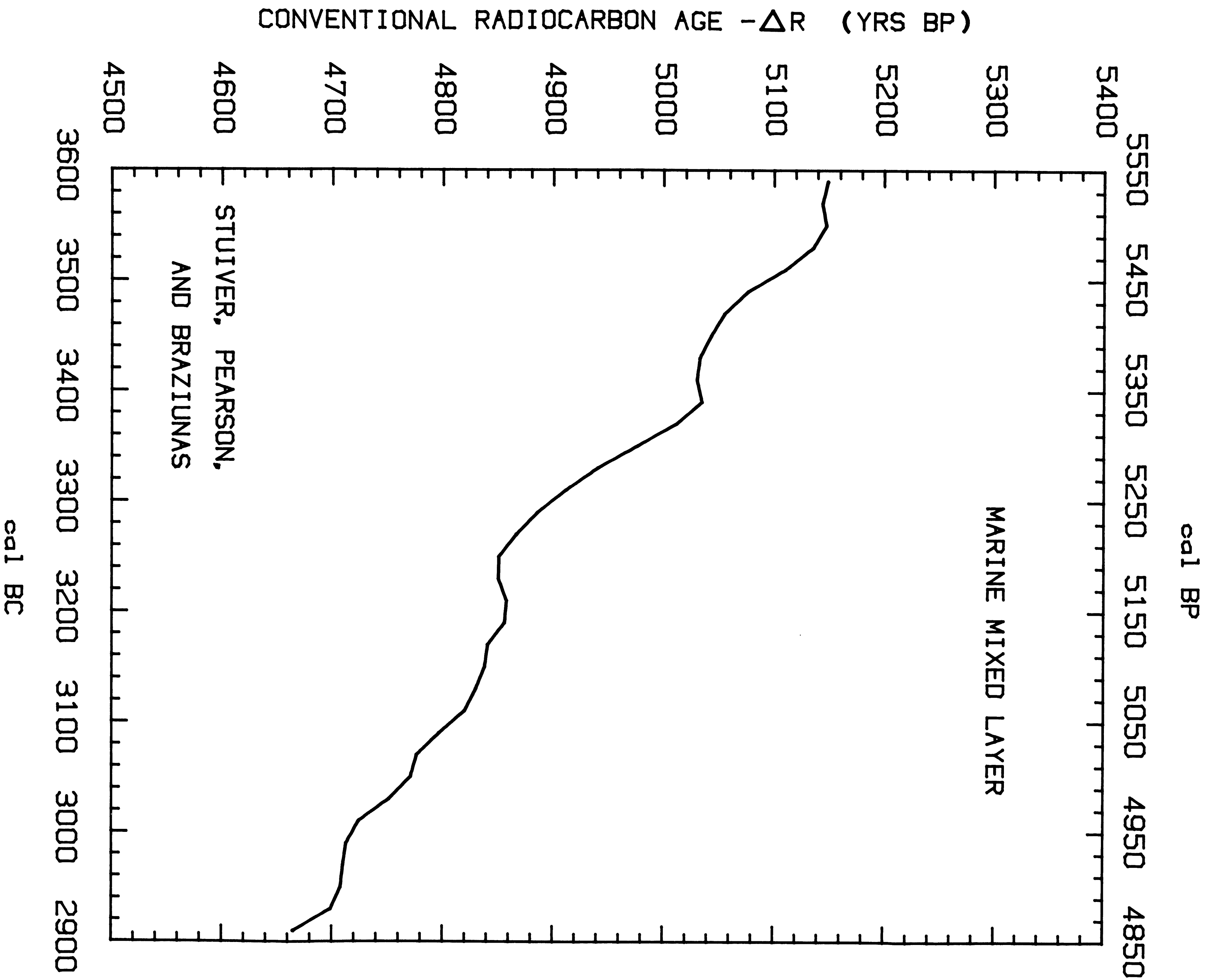

CONVENTIONAL RADIOCARBON AGE -ΔR (YRS BP)
4500
4600
4700
4800
4900
5000
5100
5200
5300
5400
cal BP
5550
5450
5350
5250
5150
5050
4950
4850
cal BC
3600
3500
3400
3300
3200
3100
3000
2900
STUIVER, PEARSON,
AND BRAZIUNAS
MARINE MIXED LAYER

Fig 11K

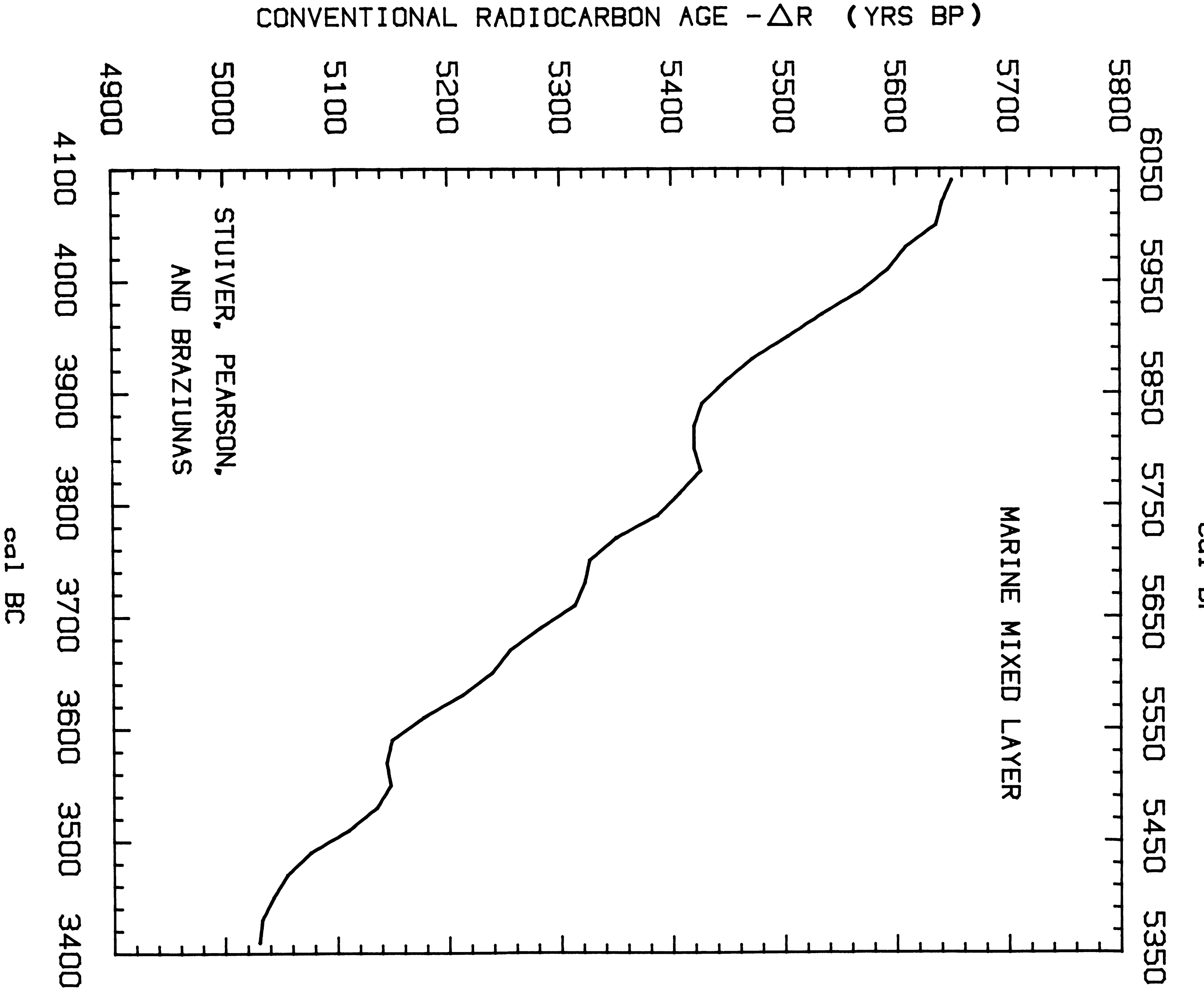
CONVENTIONAL RADIOCARBON AGE -ΔR (YRS BP)
4900
5000
5100
5200
5300
5400
5500
5600
5700
5800
cal BP
6050
5950
5850
5750
5650
5550
5450
5350
MARINE MIXED LAYER
STUIVER, PEARSON,
AND BRAZIUNAS
cal BC
4100
4000
3900
3800
3700
3600
3500
3400

Fig 11L

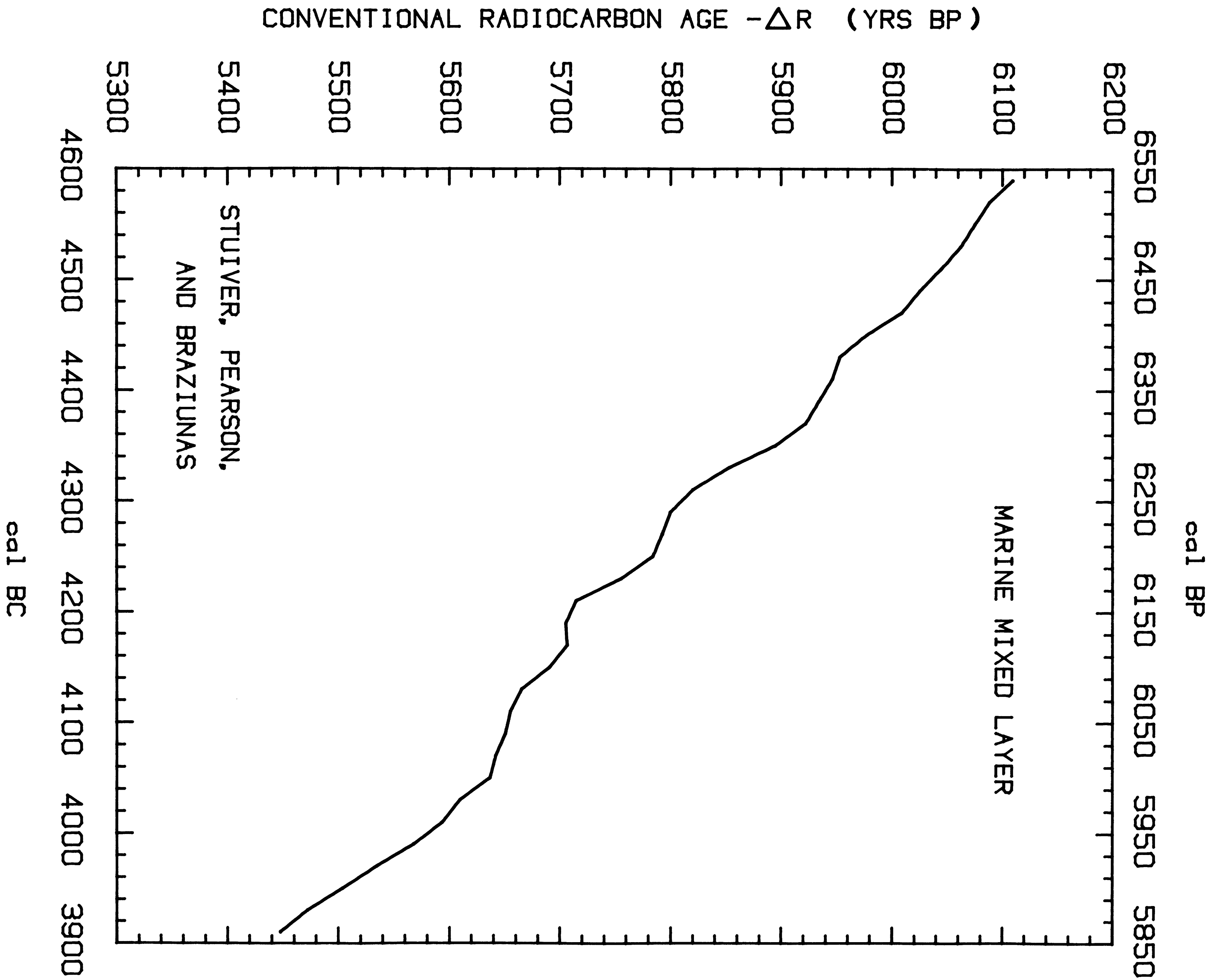
CONVENTIONAL RADIOCARBON AGE -ΔR (YRS BP)
5300
5400
5500
5600
5700
5800
5900
6000
6100
6200
cal BP
6550
6450
6350
6250
6150
6050
5950
5850
cal BC
4600
4500
4400
4300
4200
4100
4000
3900
MARINE MIXED LAYER
STUIVER, PEARSON, AND BRAZIUNAS

Fig 11M

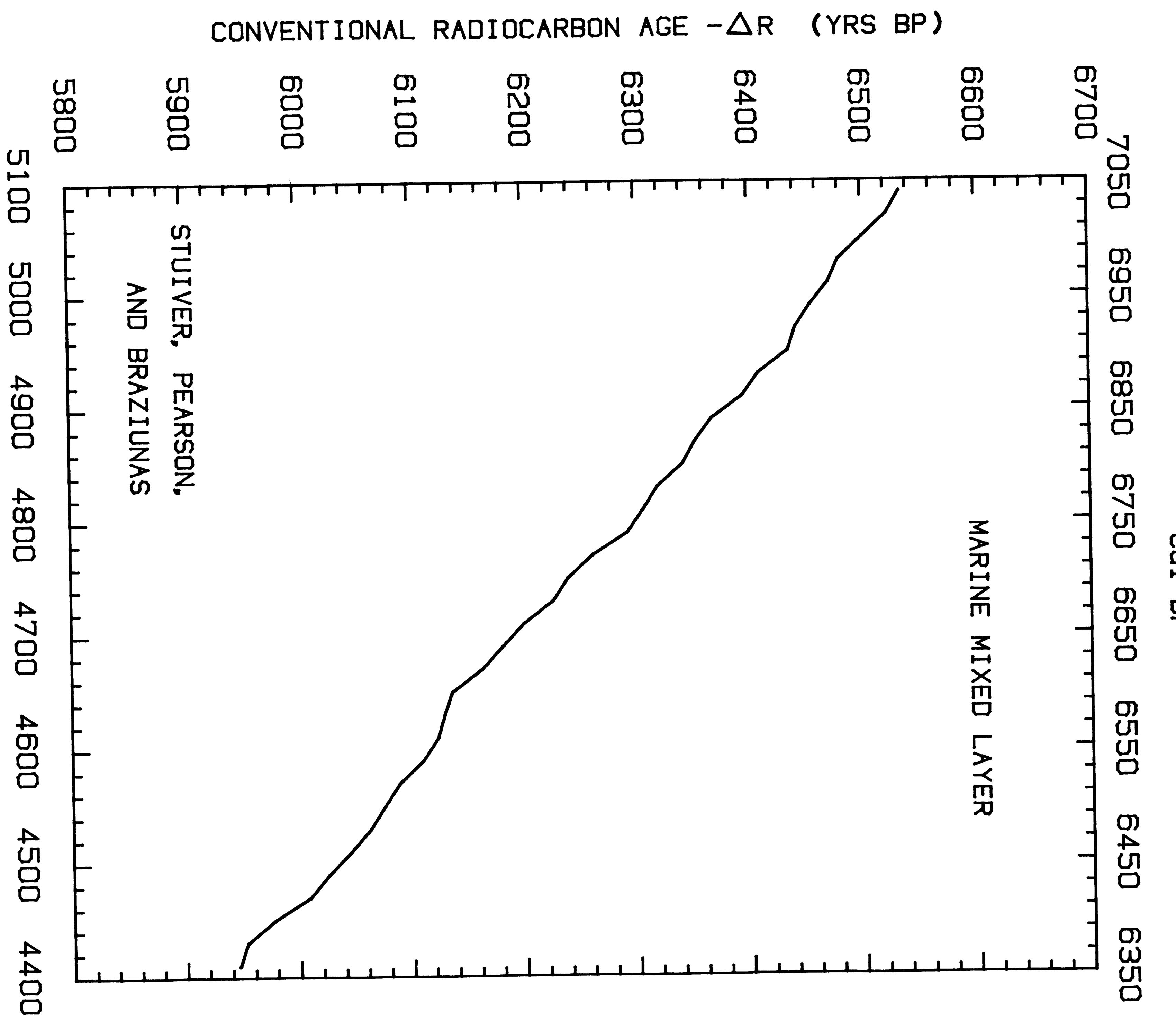

CONVENTIONAL RADIOCARBON AGE -ΔR (YRS BP)
5800
5900
6000
6100
6200
6300
6400
6500
6600
6700
cal BP
7050
6950
6850
6750
6650
6550
6450
6350
cal BC
5100
5000
4900
4800
4700
4600
4500
4400
STUIVER, PEARSON, AND BRAZIUNAS
MARINE MIXED LAYER

Fig 11N

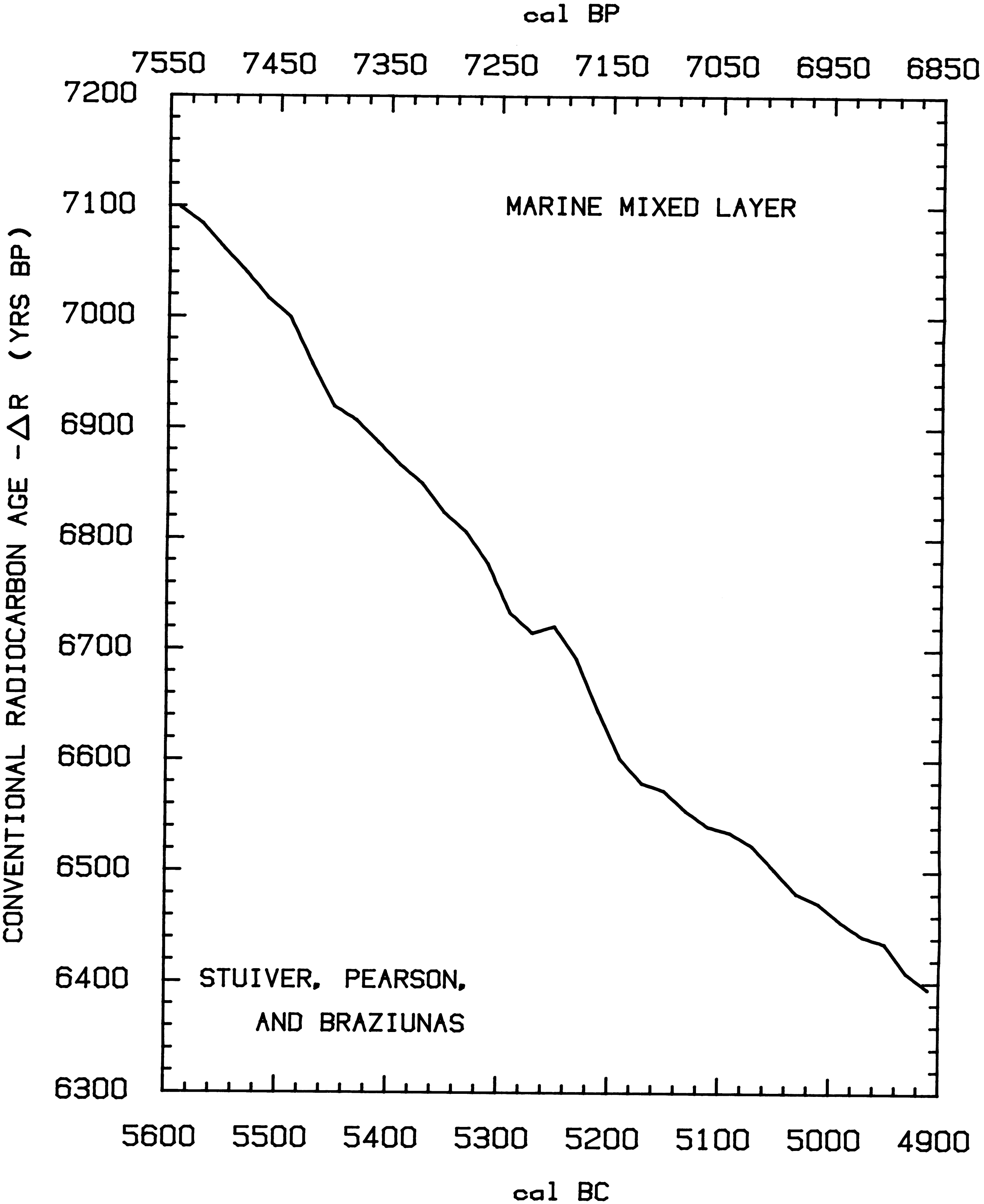
cal BP
7550
7450
7350
7250
7150
7050
6950
6850
CONVENTIONAL RADIOCARBON AGE -ΔR (YRS BP)
7200
7100
7000
6900
6800
6700
6600
6500
6400
6300
MARINE MIXED LAYER
STUIVER, PEARSON,
AND BRAZIUNAS
5600
5500
5400
5300
5200
5100
5000
4900
cal BC
Fig 11O

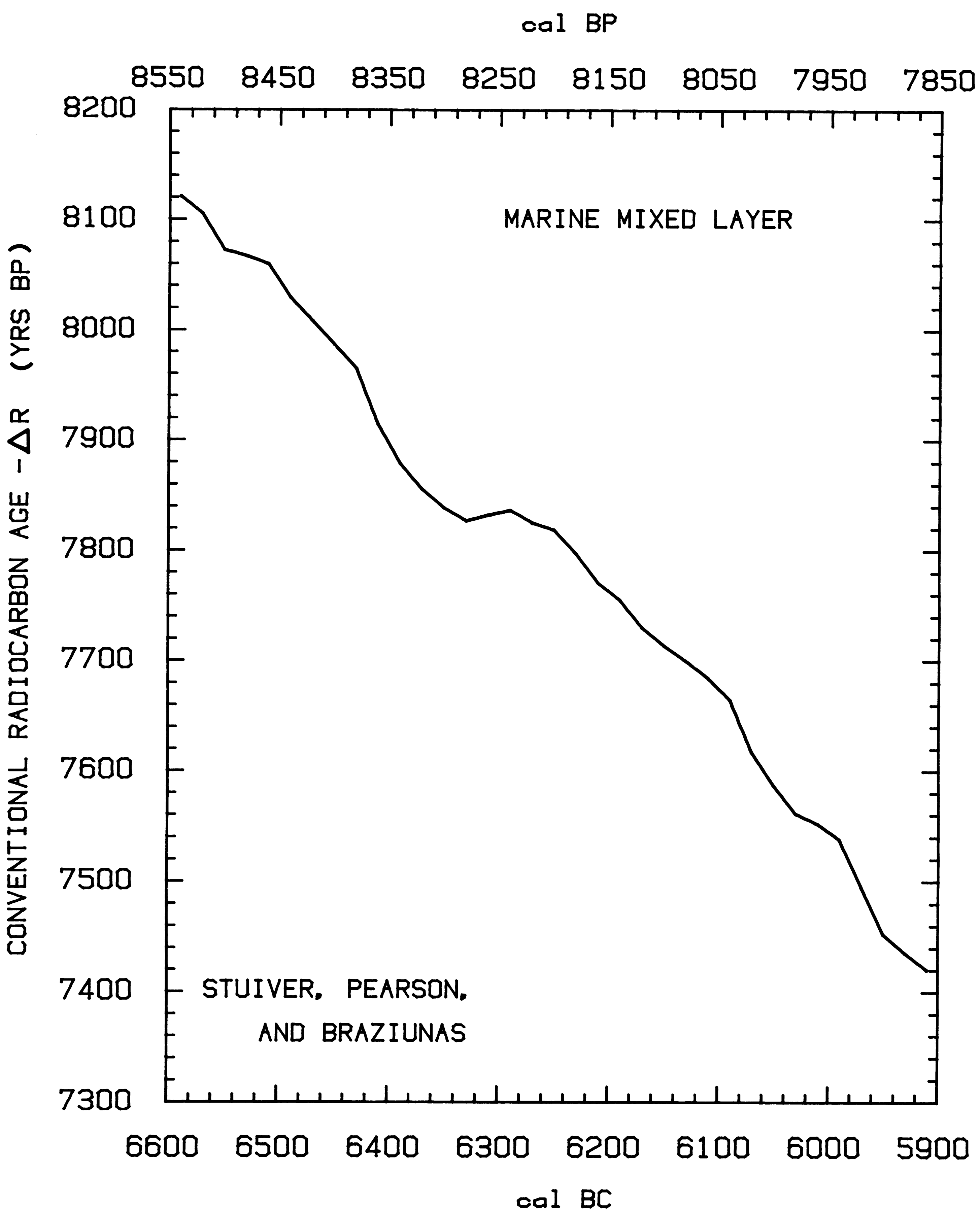
cal BP
8550
8450
8350
8250
8150
8050
7950
7850
CONVENTIONAL RADIOCARBON AGE -ΔR (YRS BP)
8200
8100
8000
7900
7800
7700
7600
7500
7400
7300
MARINE MIXED LAYER
STUIVER, PEARSON,
AND BRAZIUNAS
6600
6500
6400
6300
6200
6100
6000
5900
cal BC
Fig 11Q

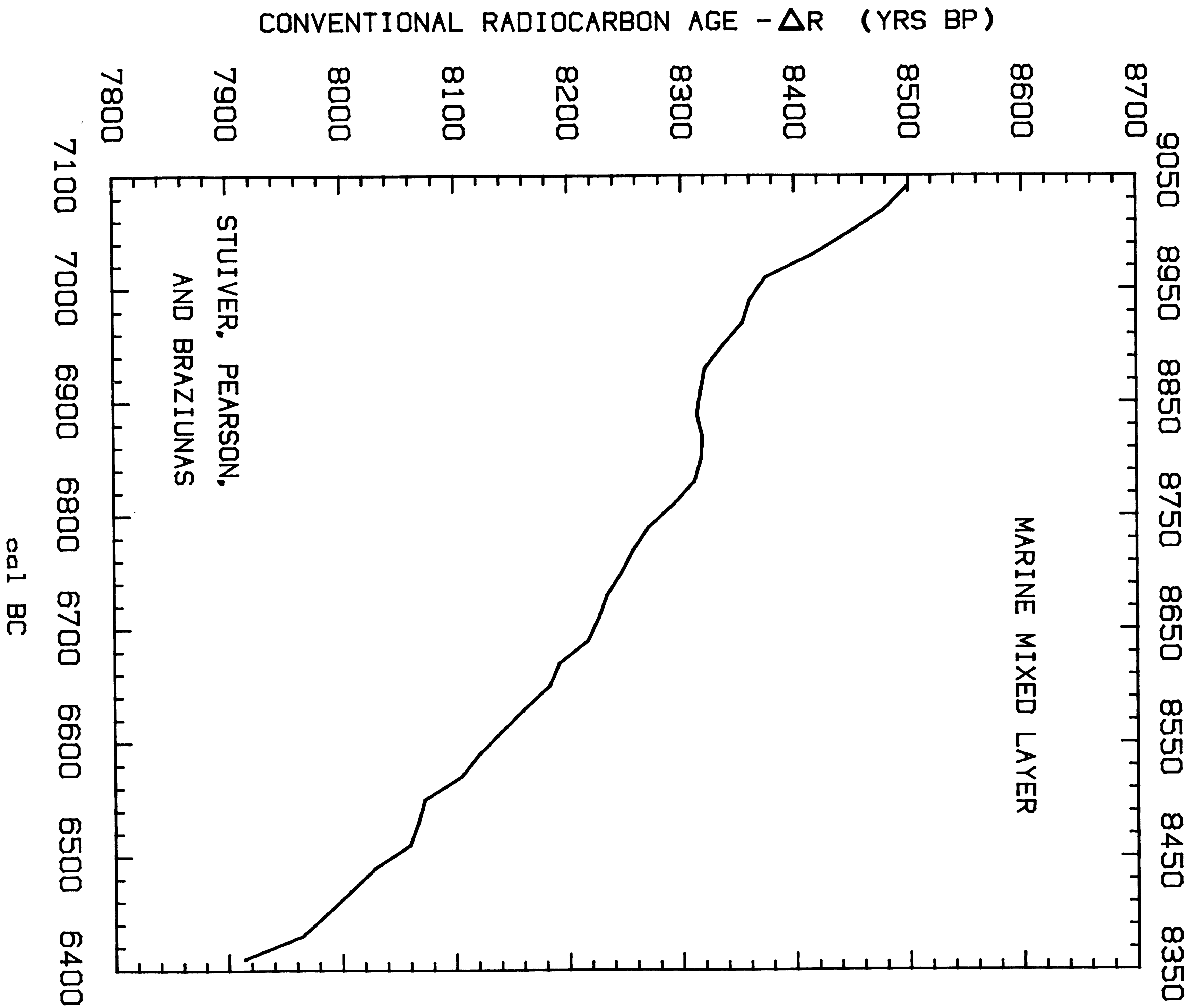
CONVENTIONAL RADIOCARBON AGE -ΔR (YRS BP)
7800
7900
8000
8100
8200
8300
8400
8500
8600
8700
cal BP
9050
8950
8850
8750
8650
8550
8450
8350
MARINE MIXED LAYER
STUIVER, PEARSON, AND BRAZIUNAS
cal BC
7100
7000
6900
6800
6700
6600
6500
6400

Fig 11R

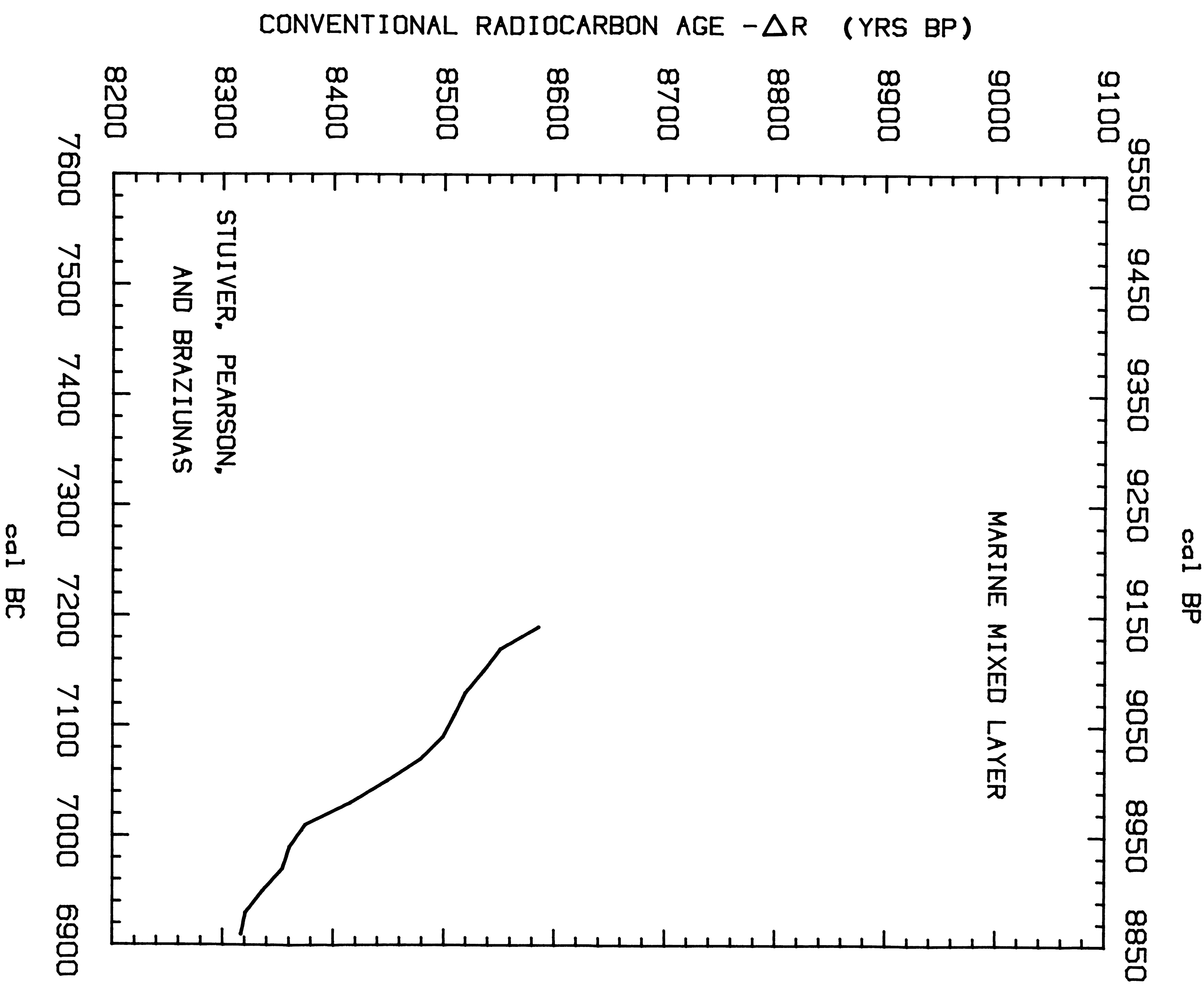

CONVENTIONAL RADIOCARBON AGE -ΔR (YRS BP)
8200
8300
8400
8500
8600
8700
8800
8900
9000
9100
cal BP
9550
9450
9350
9250
9150
9050
8950
8850
MARINE MIXED LAYER
STUIVER, PEARSON,
AND BRAZIUNAS
cal BC
7600
7500
7400
7300
7200
7100
7000
6900

Fig 11S

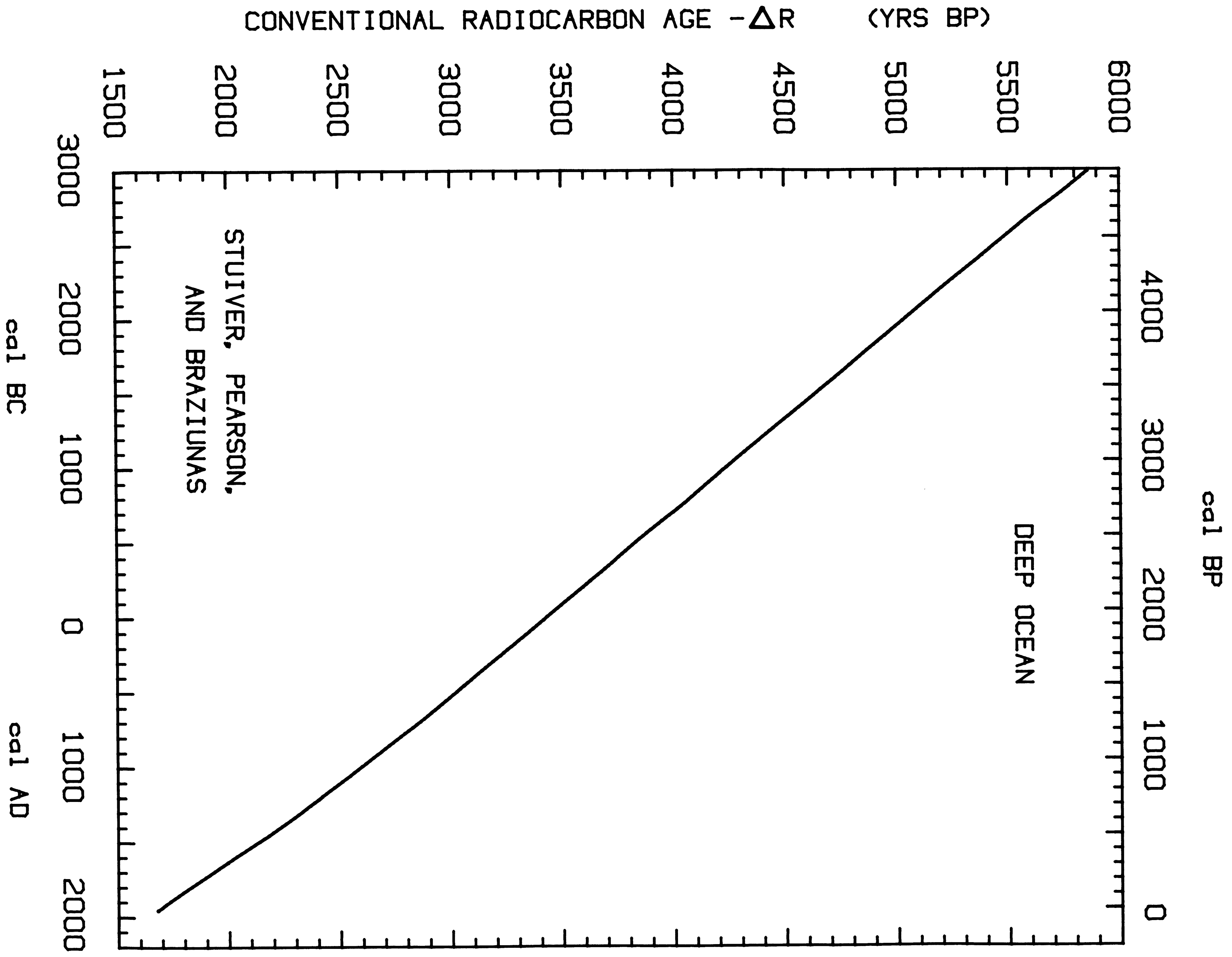

Fig 12. Deep ocean conventional ^{14}C ages *vs* cal AD/BC (cal BP) ages. ΔR is discussed in the text.

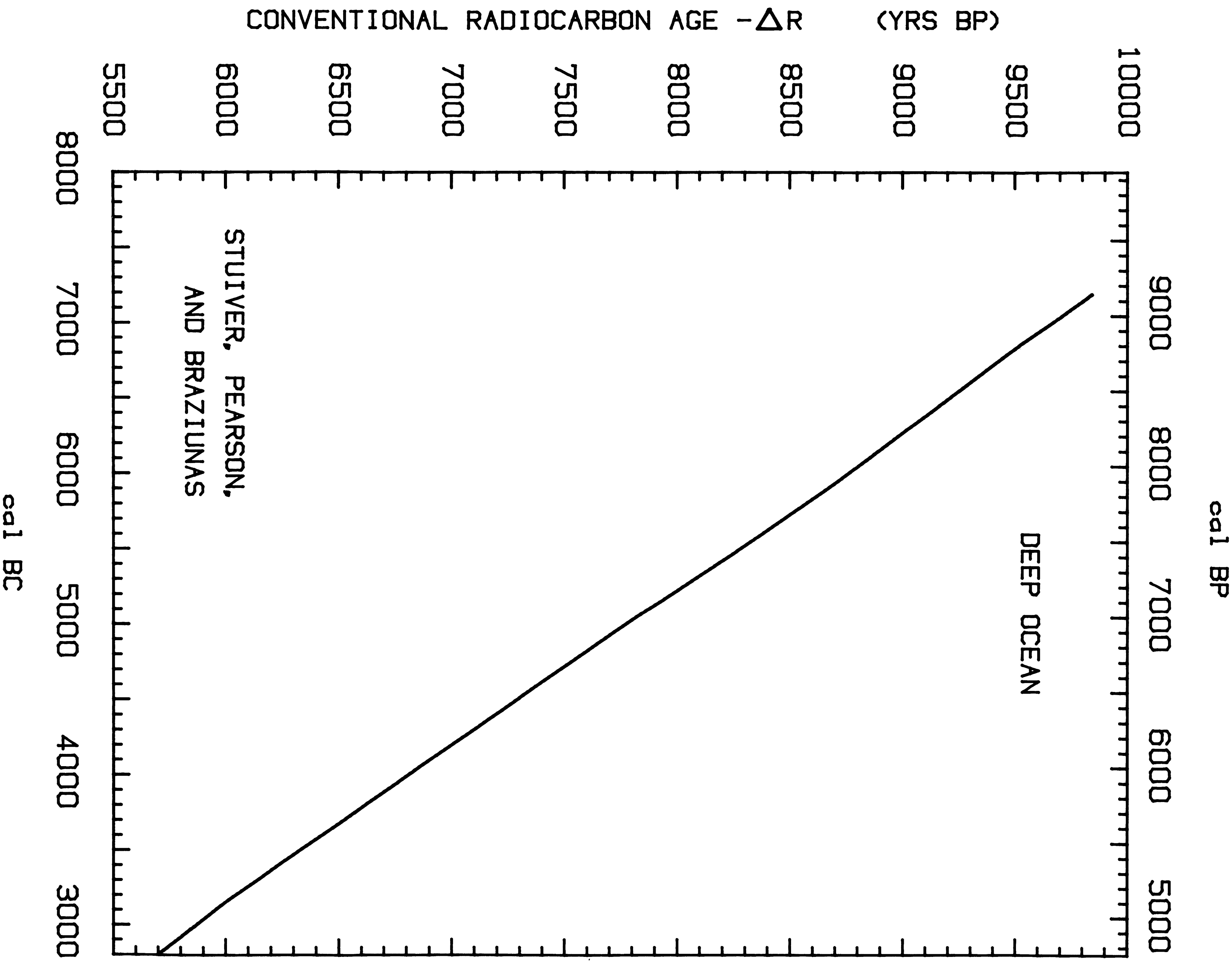
CONVENTIONAL RADIOCARBON AGE -ΔR (YRS BP)
5500
6000
6500
7000
7500
8000
8500
9000
9500
10000
cal BP
9000
8000
7000
6000
5000
cal BC
8000
7000
6000
5000
4000
3000
DEEP OCEAN
STUIVER, PEARSON,
AND BRAZIUNAS

Fig 12B

TABLE 1
Marine radiocarbon ages and ΔR values of mostly shell samples of known historic age

MARINE SHELLS[a] REF[b]	REGION[c]	SAMPLE #	HISTORICAL AGE (cal AD)[d]	CONVENTIONAL SAMPLE ^{14}C AGE (^{14}C YRS BP)[e]	ΔR (^{14}C YRS BP)[f]
11,9	Diabasvika, Lagoya, Spitsbergen 80°34'N 18°35'E	U-121	1958[g]	670±80	180±80[h]
11,9	NE side of Nordre, Russoya, Murchisonfjorden, Spitsbergen 80°0'N 18°9'E	U-122	1958[g]	430±80	-60±80[h]
10	Magdalenafj., Spitsbergen 79°34'N 10°40'E	T-1541	1878	632±70	141±70
11,9	Tangen, Mushamna, Spitsbergen 79°30'N 14°E	U-133	1952[g]	530±70	40±60[h]
10	Adventbukta, Spitsbergen 78°15'N 15°36'E	T-1540	1878	622±70	131±70
10	Isfjorden, Spitsbergen 78°07'N 14°08'E	T-1539	1925	519±50	45±50
10	Bellsund, Spitsbergen ca. 77°40'N 14-16°E	T-1538	1926	549±50	75±50
10	Near Bear Island 74°07'N 19°04'E	T-1537	1900	523±50	46±50
	WEIGHTED MEAN OF ABOVE 8 SAMPLES SCATTER σ IN UNWEIGHTED MEAN IS 25 YR				70±20
10	Rice Strait, Smith Sound, Ellesmere Island 78°45'N 74°55'E	T-1544	1898	744±70	266±70
10	Goose Bay, Jones Sound, Ellesmere Island ca. 76°45'N 89°00'E	T-1543	1900	893±70	416±70
10	Havnefjorden, Jones Sound, Ellesmere Island 76°30'N 84°30'E	T-1542	1899	774±70	297±70
	WEIGHTED MEAN OF ABOVE 3 SAMPLES SCATTER σ IN UNWEIGHTED MEAN IS 45 YR				325±40
8	S of L. Pendulumoen and SE of Claveringoen, NE Greenland 74°35'N 18°23'W and 74°10'N 20°08'W	Lu-650	1899	591±38	114±38
8	Mackenziebugt, NE Greenland 73°28'N 21°30'W	Lu-609	1900	650±47	173±47
8	Mackenziebugt, NE Greenland 73°28'N 21°30'W	Lu-610	1900	620±54	143±54

TABLE 1 (continued)

MARINE SHELLS[a]

REF[b]	REGION[c]	SAMPLE #	HISTORICAL AGE (cal AD)[d]	CONVENTIONAL SAMPLE ^{14}C AGE (^{14}C YRS BP)[e]	ΔR (^{14}C YRS BP)[f]
8	Fame Oer, Scoresby Sund, NE Greenland 70°50′N 22°33′W	Lu-643	1899	641±39	164±39
17	S cove, Nyhavn, NE Greenland (ca. 72°N 23°W)	Y-606	1957	550±70	60±70[h]
	WEIGHTED MEAN OF ABOVE 5 SAMPLES SCATTER σ IN UNWEIGHTED MEAN IS 20 YR				140±20
10	Tanafjord, Finnmark, N Norway 70°30′-71° N ca. 28°30′E	T-1535	1876	584±70	91±70
9	Komagfjord, Finnmark, N Norway 70°16′N 23°24′E	T-958	1922	548±75	75±75
10	Vadso, Finnmark, N Norway 70°04′N 29°45′E	T-1536	1857	543±50	41±50
10	Tromso, Troms, N Norway 69°39′N 18°58′E	T-1534	1857	553±50	51±50
	WEIGHTED MEAN OF ABOVE 4 SAMPLES SCATTER σ IN UNWEIGHTED MEAN IS 10 YR				60±30
3	Faxa Bay, Kollafjord, Iceland 64°N 22°W	L-576C	1946	543±51	56±51
3	Faxa Bay, Kollafjord, Iceland 64°N 22°W	L-576H	1900	631±51	154±51
3	Faxa Bay, Kollafjord, Iceland 64°N 22°W	L-576I	1840	715±51	203±51
	WEIGHTED MEAN OF ABOVE 3 SAMPLES SCATTER σ IN UNWEIGHTED MEAN IS 45 YR				140±30
9	Fjaerlandsfjorden, Sogn, Norway Btwn 61°13′N 6°34′E and 61°22′N 5°00′E	T-953	1909	541±80	70±80
9	Leikanger, Sognefjord, Norway 61°11′N 6°48′E	T-951	1912	438±75	-33±75
9	Vangsnes, Sognefjord, Norway 61°10′N 6°39′E	T-952	1920	500±75	27±75
9	North Sea, approx. half way btwn Bergen and Shetland 60°38′N 2°35′E	T-957	1906	494±75	21±75
10	Vikingbank, North Sea 60°38′N 2°35′E	T-1533	1906	469±50	-4±50
9	Ideosen, Herdla, Hordaland, Norway 60°34′N 5°00′E	T-954A, T-954B	1923	457±60	-16±60
9	Sollesnes, Jondal, Hardanger, Norway 60°18′N 6°17′E	T-955	1908	532±75	61±75
9	Mosterhavn, Hordaland, Norway 59°42′N 5°24′E	T-956	1918	402±90	-70±90
	WEIGHTED MEAN OF ABOVE 8 SAMPLES SCATTER σ IN UNWEIGHTED MEAN IS 15 YR				5±25
9	Brevikfjord, Telemark, Norway 59°03′N 9°42′E	T-959	1898	602±80	124±80
9	Gronholmsund, Risor, Aust-Agder, Norway 58°44′N 9°18′E	T-960	1905	385±75	-88±75
7	Near Kristingeberg, island of Skaftolandet, Bohuslan, Sweden 58°15′N 11°26′E	Lu-237	1896±8[g]	420±50	-59±50
12	Bohuslan, Sweden (ca. 58°N 12°E)	U-607	ca.1935	510±80	31±80
6	Haron, Bohuslan, Sweden 58°01′N 11°31′E	Lu-236	1935±15	430±46	-49±46
6	Roro, N archipelago of Goteborg, Sweden 57°47′N 11°37′E	Lu-235	1930±10	410±46	-65±46
6	Roro, N archipelago of Goteborg, Sweden 57°47′N 11°37′E	Lu-234	1930±10	370±57	-105±57
10	Skagerak, Norway 57°44′N 9°53′E	T-1532	1906	459±50	-14±50
	WEIGHTED MEAN OF ABOVE 8 SAMPLES SCATTER σ IN UNWEIGHTED MEAN IS 25 YR				-40±20
14	Pavlov Harbor, Alaska, USA 55.5°N (162°W)	USGS-234	1937	700±50	219±50
	VALUE USED ON MAP FOR ABOVE SAMPLE				220±50
14	Orcas Is., Washington, USA 48.6°N (123°W)	USGS-177	1915±15	805±50	334±50
14	Orcas Is., Washington, USA 48.6°N (123°W)	USGS-190	1915±15	950±30	479±30

Table 1 (continued)

MARINE SHELLS[a] REF[b]	REGION[c]	SAMPLE #	HISTORICAL AGE (cal AD)[d]	CONVENTIONAL SAMPLE ^{14}C AGE (^{14}C YRS BP)[e]	ΔR (^{14}C YRS BP)[f]
14	Sooke, British Columbia, Canada 48.4°N (124°W)	USGS-170	1916	850±50	378±50
14	Esquimalt, British Columbia Canada 48.3°N (123°W)	USGS-133	1930	750±50	275±50
14	Yaquina Bay, Oregon, USA 44.6°N (124°W)	USGS-169	1916	840±35	368±35
14	Yaquina Bay, Oregon, USA 44.6°N (124°W)	USGS-189	1916	835±50	363±50
14	Sunset Bay, Oregon, USA 43.3°N (124°W)	USGS-233	1936	895±50	415±50
	WEIGHTED MEAN OF ABOVE 7 SAMPLES SCATTER σ IN UNWEIGHTED MEAN IS 25 YR				390±15
3	Bay of Arcachon, France 44°35′N 1°25′W	L-599A	1952	846±42	-4±42[h]
	VALUE USED ON MAP FOR ABOVE SAMPLE				-5±40
2,3	Port Jefferson area, Long Island Sound, New York, USA 40°57′N 73°05′W	L-317A	1954	407±75	-83±75[h]
	VALUE USED ON MAP FOR ABOVE SAMPLE				-85±75
14	Bolinas Bay, California, USA 37.9°N (123°W)	USGS-248	1915±5	680±25	209±25
14	Half Moon Bay, California, USA 37.5°N (122°W)	USGS-280	1915±5	745±35	274±35
14	Monterey, California, USA 36.6°N (122°W)	USGS-178	1915±5	740±35	269±35
1	Monterey, California, USA (37°N 122°W)	UCLA-149	1878	566±55	75±55
14	Morro Bay, California, USA 35.4°N (121°W)	USGS-281	1947	750±35	262±35
1	Seal Beach, California, USA (34°N 119°W)	UCLA-1033	1921	553±48	80±48
14	San Diego, California, USA 32.7°N (117°W)	USGS-430	1915±5	735±35	264±35
	WEIGHTED MEAN OF ABOVE 7 SAMPLES SCATTER σ IN UNWEIGHTED MEAN IS 35 YR				225±15

Table 1 (continued)

MARINE SHELLS[a] REF[b]	REGION[c]	SAMPLE #	HISTORICAL AGE (cal AD)[d]	CONVENTIONAL SAMPLE ^{14}C AGE (^{14}C YRS BP)[e]	ΔR (^{14}C YRS BP)[f]
2,3	Kouali Point, Tipasa, Algeria 36°40′N 2°30′E	L-241A	1954	357±83	-133±83[h]
	VALUE USED ON MAP FOR ABOVE SAMPLE				-135±85
1	Kino Bay, Sonora, Mexico (29°N 112°W)	UCLA-914	1935	993±53	514±53
1	Carmen Is., Gulf of California, Mexico (26°N 111°W)	UCLA-917	1911	1001±54	531±54
	WEIGHTED MEAN OF ABOVE 2 SAMPLES SCATTER σ IN UNWEIGHTED MEAN IS 10 YR				520±40
1	Cedro Is., Baja California, Mexico (28°N 115°W)	UCLA-963	1939	614±51	132±51
1	Magdaleno Bay, Baja California, Mexico (25°N 112°W)	UCLA-939	1938	660±53	179±53
1	Cape San Lucas, Baja California, Mexico (23°N 110°W)	UCLA-916	1932	784±45	307±45
1	Mazatlan, Sinaloa, Mexico (23°N 106°W)	UCLA-913	1939	662±48	180±48
1	Isabel Island, Nayarit, Mexico (22°N 106°W)	UCLA-936	1938	688±50	207±50
1	Banderas Bay, Jalisco, Mexico (21°N 105°W)	UCLA-940	1938	606±50	125±50
1	Manzanillo, Colima, Mexico (19°N 104°W)	UCLA-915	1930	675±50	200±50
1	Guatulco Bay, Oaxaca, Mexico (16°N 96°W)	UCLA-938	1938	621±50	140±50
	WEIGHTED MEAN OF ABOVE 8 SAMPLES SCATTER σ IN UNWEIGHTED MEAN IS 20 YR				185±15
3	Bahama Islands 26°N 78°W	L-576B	1950	428±42	-62±42
3	Bahama Islands 26°N 78°W	L-576G	1885±5	525±59	39±59

TABLE 1 (continued)

MARINE SHELLS[a] REF[b]	REGION[c]	SAMPLE #	HISTORICAL AGE (cal AD)[d]	CONVENTIONAL SAMPLE ^{14}C AGE (^{14}C YRS BP)[e]	ΔR (^{14}C YRS BP)[f]
4	The Rocks, offshore of Florida Keys, USA 24°57'N 80°33'W	(annual coral rings)	"1850" (1800-1900)	518±16	13±16
3	Jamaica, B.W.I. 18°N 78°W	L-576A	1929-1930	423±42	-52±42
3	Jamaica, B.W.I. 18°N 78°W	L-576F	1884	425±41	-62±41
	WEIGHTED MEAN OF ABOVE 5 SAMPLES SCATTER σ IN UNWEIGHTED MEAN IS 20 YR				-5±15
3	Oahu, Hawaii, USA 22°N 158°W	L-576J	1840-1841	629±51	117±51
	VALUE USED ON MAP FOR ABOVE SAMPLE				115±50
3	Off Bogan Island, Eniwetok Atoll 11°30'N 162°10'E	L-584A (coral)	1946	629±43	142±43
	VALUE USED ON MAP FOR ABOVE SAMPLE				140±45
16	Port Parker, Costa Rica (ca. 10°N 85°W)	UCLA-1254	1935	695±37	216±37
16	Secas Island, Panama (8°N 82°W)	UCLA-1256A	1934	403±51	-76±51
16	Secas Island, Panama (8°N 82°W)	UCLA-1256B	1935	507±49	28±49
16	Santiago Is., Galapagos Is. (0°N 91°W)	UCLA-1255A	1934	538±53	60±53
16	Santiago Is., Galapagos Is. (0°N 91°W)	UCLA-1255B	1934	745±82	267±82
16	Espanola Is., Galapagos Is. (0°N 90°W)	UCLA-1255C	1934	468±43	-10±43
16	Santa Cruz Is., Galapagos Islands (0°N 90°W)	UCLA-1255D	1932	443±40	-34±40
16	Guayaquil, Ecuador (ca. 3°S 80°W)	UCLA-1249A	1927	235±37	-240±37
16	Guayaquil, Ecuador (ca. 3°S 80°W)	UCLA-1249B	1927	536±45	61±45
	WEIGHTED MEAN OF ABOVE 9 SAMPLES SCATTER σ IN UNWEIGHTED MEAN IS 50 YR				5±15

TABLE 1 (continued)

MARINE SHELLS[a] REF[b]	REGION[c]	SAMPLE #	HISTORICAL AGE (cal AD)[d]	CONVENTIONAL SAMPLE ^{14}C AGE (^{14}C YRS BP)[e]	ΔR (^{14}C YRS BP)[f]
16	Northern Peru (ca. 10°S 80°W)	UCLA-1282	1935±5	700±49	221±49
16	Peru (ca. 14°S 78°W)	UCLA-1279	1935±5	1127±44	648±44
16	Antofagasta, Chile (24°S 70°W)	UCLA-1277	1925	626±34	152±34
16	Valparaiso, Chile (33°S 72°W)	UCLA-1278	1935±5	770±76	291±76
	WEIGHTED MEAN OF ABOVE 3 SAMPLES (WITH UCLA-1279 EXCLUDED) SCATTER σ IN UNWEIGHTED MEAN IS 40 YR				190±25
5	Torres Strait, Australian coast ca. 10°S 143°E	SUA-354/1	1875±3	480±67	-13±67
5	Torres Strait, Australian coast ca. 10°S 143°E	SUA-354/2	1875±3	463±84	-30±84
5	Torres Strait, Australian coast ca. 10°S 143°E	SUA-357	1909	404±84	-67±84
5	Garden Island, W. Australia 32°15'S 115°40'E	SUA-355	1930	454±84	-21±84
5	Adelaide, S. Australia ca. 35°S 139°E	SUA-393	1937±2	583±85	102±85
5	Narooma, N.S.W. Australia 36°13'S 150°07'E	SUA-356	1950	480±84	-10±84
	WEIGHTED MEAN OF ABOVE 6 SAMPLES SCATTER σ IN UNWEIGHTED MEAN IS 25 YR				-5±35
3	Tahiti 18°S 149°W	L-576E	1957	515±42	25±42[h]
3	Moorea 18°S 149°W	L-576K	1883±3	553±42	65±42
	WEIGHTED MEAN OF ABOVE 2 SAMPLES SCATTER σ IN UNWEIGHTED MEAN IS 20 yr				45±30
5	New Zealand -----	----	1923	416±42	-57±42
5	New Zealand -----	----	1925	371±50	-103±50
5	New Zealand -----	----	1949	210±41	-280±41
13	Otago, New Zealand (ca. 45°S 170°E)	INS no. R.42	1955	446±42	-44±42[h]

TABLE 1 (continued)

MARINE SHELLS[a] REF[b]	REGION[c]	SAMPLE #	HISTORICAL AGE (cal AD)[d]	CONVENTIONAL SAMPLE ^{14}C AGE (^{14}C YRS BP)[e]	ΔR (^{14}C YRS BP)[f]
	WEIGHTED MEAN OF ABOVE 3 SAMPLES (WITH -280±41 EXCLUDED) SCATTER σ IN UNWEIGHTED MEAN IS 20 YR				-65±25
15	Inexpressible Island, Antarctica (ca. 74°54′S 163°39′E)	QL-171 (seal)	1912	1390±40	919±40
15	Inexpressible Island Antarctica (ca. 74°54′S 163°39′E)	QL-173 (penguin)	1912	1300±50	829±50
	WEIGHTED MEAN OF ABOVE 2 SAMPLES SCATTER σ OF UNWEIGHTED MEAN IS 45 YR				885±30

NOTES

a Exceptions are marked.

b References are: (1) Berger et al., 1966; (2) Broecker and Olson, 1959; (3) Broecker and Olson, 1961; (4) Druffel and Linick, 1978; (5) Gillespie and Polach, 1979; (6) Hakansson, 1969; (7) Hakannson, 1970; (8) Hakansson, 1973; (9) Mangerud, 1972; (10) Mangerud and Gulliksen, 1975; (11) Olsson, 1960; (12) Olsson et al., 1969; (13) Rafter et al., 1972; (14) Robinson and Thompson, 1981; (15) Stuiver et al., 1981; (16) Taylor and Berger, 1967; and (17) Washburn and Stuiver, 1962.

c Our own estimates of missing coordinates are in parentheses.

d Age refers to calendar year of death. Only pre-1959 samples are listed.

e Conventional radiocarbon age is: taken directly from original listing (references 14, 15, and 17); assumed equivalent to reported "apparent age" (references 6 and 7); calculated from reported $\delta^{14}C$ or $\Delta^{14}C$ (references 1, 13, and 16); calculated from reported $\Delta^{14}C$ after removal of age correction (references 4, 5, 8, 9, and 12); calculated from reported $\Delta^{14}C$ after removal of age correction to 1958 (references 2 and 3); or calculated from reported $\Delta^{14}C$ after removal of age correction and fossil fuel correction (reference 10 and Rafter values listed in reference 5).

f Sigma in ΔR (σ_R) is minimum error based on reported error in conventional sample ^{14}C age.

g Exact year of death is not known.

h Computation is based on the model mixed layer radiocarbon age calculated for AD 1950